THE STUDY OF RADIO REFRACTIVITY IN SELECTED STATES OF NIGERIA

BY

BALARABE, Maryam
MTech/ SPS/ 2018/ 7805

A THESIS SUBMITTED TO THE POSTGRADUATE SCHOOL FEDERAL UNIVERSITY OF TECHNOLOGY, MINNA, NIGERIA IN PARTIAL FULFILLMENT OF THE REQUIREMENTS FOR THE AWARD OF THE DEGREE OF MASTER OF TECHNOLOGY IN APPLIED ATMOSPHERIC PHYSICS

NOVEMBER, 2023

DECLARATION

I hereby declare that this thesis titled: ‘‘THE STUDY OF RADIO REFRACTIVITY IN SELECTED STATE OF NIGERIA’’ is a collection of my original research work and it has not been presented for any other qualification anywhere. Information from other sources (published or unpublished) has been duly acknowledged.

BALARABE MARYAM
MTech/SPS/2018/7805
FEDERAL UNIVERSITY OF TECHNOLOGY
NIGERIA

…..……
SIGNATURE/DATE

CERTIFICATION

The thesis titled: ‘‘THE STUDY OF RADIO REFRACTIVITY IN SELECTED STATE OF NIGERIA’’ by: BALARABE, Maryam (MTech/SPS/2018/7805) meets the regulations governing the award of the degree of (MTech) of the Federal University of Technology, Minna and it is approved for its contribution to scientific knowledge and literary presentation.

PROF. O. D. OYEDUM .....
MAJOR SUPERVISOR Signature/Date

DR. K. C. IGWE .....
CO-SUPERVISOR Signature/Date

DR. A. S. MOSES .....
HEAD OF DEPARTMENT Signature/Date

PROF. J. YISA .....
DEAN, SCHOOL OF PHYSICAL SCIENCE Signature/Date

ENGR. PROF. O. K. ABUBAKRE .....

DEAN, POSTGRADUATE SCHOOL Signature/Date

DEDICATION

This thesis is dedicated to my parents and related science lovers.

ACKNOWLEDGEMENTS

All praise to ALLAH (s.w.t) the most beneficent, the most merciful. The all-knowing and the giver of knowledge for His mercy and blessings upon me during my stay at the Federal University of Technology, Minna.

I express my sincere gratitude to my supervisor, Prof. O. D. Oyedum for his unyielding assistance, contributions and guidance rendered to me throughout the research work. I also wish to appreciate and express my gratitude to my co- supervisor Dr. K. C. Igwe for all his valuable commentaries and effort which was a great aid towards the completion of this research.

Special thanks to the H. O. D Dr. A. S. Moses and the entire staff of the Department of Physics, Federal University of Technology, who impacted knowledge and additional guidance to me.

I would also like to acknowledge the Nigerian Meteorological Agency (NIMet), Abuja and Centre for Atmospheric Research (CAR), Anyigba a unit under National Space Research and Development Agency (NASRDA).

Warm appreciation to my parents and entire family for giving me their backings and the opportunity to grow.

Lastly, my friends, course-mates and colleagues who assisted me through this journey, may Allah's blessings be with you always. Thank you.

ABSTRACT

The knowledge of radio refractivity are useful in many applications and design of radio links for communication network system, navigation, surveillance system and other radar systems for the purpose of attaining optimal performance and improving the quality of their services in the study area. This paper presents the study of radio refractivity of some selected State capitals in Northern Nigeria. The locations are Bauchi, Yola and Kano. The meteorological parameters obtained were used to compute radio refractivity, modified refractivity, refractivity gradient, k-factor and field strength variability. Atmospheric data of air temperature, atmospheric pressure and relative humidity for Bauchi and Yola were obtained from Centre for Atmospheric Research (CAR), Anyigba, a centre under National Space Research Development Agency (NASRDA), while Radiosonde data were obtained for Kano from the Nigerian Meteorological Agency (NIMet), Abuja for five years (2012-2016).The computed results show that radio refractivity values ranged from 260 N-units in February to 339 N-units in August in Bauchi, while the values of 233 N-units in January to 319 N-units in August ranged in Yola. For Kano, radio refractivity values varied between 237 N-units in February and 283 N-units in August. Modified refractivity values in Bauchi ranged between 357 M-units in February and 435 M-units in August, while the values of 327 M-units and 413 M-units were obtained in January and August respectively in Yola. In Kano, modified refractivity values ranged between 313 M-units in February and 358 M-units in August. The results reveals that low refractivity and low modified refractivity values were observed during the dry season and high values of the two parameters were obtained during the wet season. At 3 km, peak radio refractivity gradient values of -110 N-units/km in the wet season and -90 N-units/km in the dry season were observed in Bauchi, while values varying from -102 N-units/km in the wet season to -78 N-units/km in the dry season were observed in Yola. In Kano, radio refractivity gradient values of -36 N-units/km during the wet season and -28 N-units/km during the dry season were recorded. Maximum k-factor values of 1.57 in the wet season months and 1.70 in the dry season months were obtained in Bauchi, while values of 1.50 in the wet season months and 1.65 in the dry season months were obtained in Yola. For Kano, k-factor values ranged from 1.22 during the wet season to 1.30 during the dry season. Effective earth radius factor describes how to regulate line-of-sight links in a given environment. The computed results for radio refractivity gradient and k-factor indicate that abnormal propagation condition of super-refraction occurred in Bauchi and Yola, while sub-refraction occurred in Kano. Sub-refraction leads to fading in radio communication links and reduces signal power at the receiving end, while super-refraction increases the range at which a target may be detected. The values of field strength variability computed varied from 11 dB to 12 dB in Bauchi, while values ranged from 13 dB to 16 dB in Yola. In Kano values ranging between 3 dB and 4 dB were observed. High variability leads to unstable signal power, while low variability ensures a stable signal power. Field strength variability (FSV) values were observed to be low during the wet season and high during the dry

season. The installation of more upper air and weather stations across Nigeria is important for determining radio refractivity values.

TABLE OF CONTENTS

LIST OF TABLES

LIST OF FIGURES

LIST OF ABBREVIATIONS

$\pm$	Plus or Minus
atm	Atmosphere
Atmos	Vapour
A/m	Ampere per metre
A/m^2	Ampere per square metre
ANOVA	Statistics and Linear Regression and Analysis of Variance
C	Charge
c	Constant Speed
c_p	Constant Pressure Specific Heat
C/m^2	Coulombs per metre squared
C/m^3	Coulombs per cubic metre
CAR	Centre for Atmospheric Research
℃	Centigrade
CD	Coefficient of Determination
CM-SAF	Satellite Application Facility on Climate Monitoring
$dN/_{dh}$	Refractivity Gradient
ELF	Extremely Low Frequency

EHF	Extremely High Frequency
°F	Fahrenheit
FSV	Field Strength Variability
FM	Frequency Modulation
G	Earth Surface Gravitational Acceleration
G_e	Equivalent Gradient
GHz	Giga Hertz
hPa	hectopascal
HF	High Frequency
ICAO	International Civil Aviation Organisation
ISA	International Standard Atmosphere
ISS	Integrated Sensor Suite
ITU-R	International Telecommunication Union Recommendation
K	Potential Refractive Index
K	Kelvin
kPa	Kilopascal
k-factor	Effective Earth Radius Factor
km	Kilometre
km^2	Kilometre Square
L	Temperature Lapse Rate
LF	Low Frequency
mb	Millibar
M	Molar Mass of Dry Air

M	Modified Refractivity
MF	Medium Frequency
MHz	Mega Hertz
M	Metre
mm	Millimetre
mm Hg	Millimetre of Mercury
MSL	Mean Sea Level
n	Radio Refractive Index of Air
ΔN	Refractivity Gradient
N/m^2	Newton per Square Metre
N	Newton
N	Radio Refractivity
NL	Radio Refractivity in Low level
Nm	Radio Refractivity in Mid-level
Nu	Radio Refractivity in Upper level
NTA	Nigeria Television Authority
NASRDA	National Space Research and Development Agency
NiMet	Nigeria Meteorological Agency
%	Percentage
N_s	Surface Radio Refractivity
p_0	Sea level standard atmospheric pressure
Pa	Pascal
QNH	Question Nill Height

R_0	Universal Gas Constant
R_hL	Relative Humidity in Low level
R_hm	Relative Humidity in Mid-level
R_hu	Relative Humidity in Upper level
RF	Radio Frequency
RRG	Radio Refractivity Gradient
RH	Relative Humidity
SI	Standard Unit
Sphaira	Ball or Sphere
SLF	Super Low Frequency
SHF	Super High Frequency
T	Tesla
T_0	Sea Level Standard Temperature
TL	Temperature in Low level
Tm	Temperature in Mid-level
Tu	Temperature in Upper level
THF	Tremendously High Frequency
TRODAN	Tropospheric Data Acquisition Network
UHF	Ultra-High Frequency
ULF	Ultra-Low Frequency
USA	United States of America
UV	Ultraviolet
VHF	Very High Frequency
VLF	Very Low Frequency

V/m Volts per metre

CHAPTER ONE

INTRODUCTION

1.1 Background to the Study

The atmosphere over the earth is a dynamic medium, its properties varies with atmospheric parameters such as temperature, dew point, pressure and relative humidity. The troposphere is the lowest region of the atmosphere and it extends from the earth's surface to a height of about 10 km at the middle latitudes, 6 km at the poles and about 18 km at the equator (Troposphere, 2020).This region exerts a considerable influence on radio waves at frequencies above 30 MHz, although this effect become significant only at frequencies greater than 100 MHz especially in the lower atmosphere (Hall, 1980).

Since these variables vary considerably daily and seasonally, especially in the tropics, quantitative knowledge of refractivity variations is required in order to be able to design reliable and efficient radio communication (terrestrial and satellite) systems. In radio propagation study, the troposphere is considered as a dielectric medium. Tropospheric radio refractivity poses a major setback to the free-air of communication globally. The interaction between some tropospheric factors and radio signals at frequencies > 30 MHz exposes the signals to important propagation characteristics which often degrade the communication links, especially at higher frequencies (Oyedum, 2009).

Korak-Shaha opined that the propagation of electromagnetic waves in the atmosphere (especially the troposphere) is greatly influenced by the composition of the atmosphere, and he attributed this to the fluctuations of atmospheric parameters such as temperature, dew point, pressure and relative humidity (Korak-Shaha, 2003). The tropospheric refractive index is a function of pressure, temperature and humidity and this implies that fluctuations of these atmospheric parameters (pressure, dew point, temperature and humidity) do cause significant variation in the refractive index of the air in the troposphere (Okpani *et al*., 2015).

An appropriate procedure is required for proper planning of terrestrial and earth-space radio links; this is important for assessing the refractivity effects on signals (Afullo and Odedina, 2004). The propagation of electromagnetic waves around the earth is influenced by the properties of the earth and the atmosphere (International Telecommunication Union Recommendation (ITU-R), 2019). The earth is an inhomogeneous body whose electromagnetic properties vary considerably as we go from one point to another. According to ITU-R Recommendation P.453-14 (ITU-R, 2019) the propagation loss on a terrestrial line-of-sight path relative to free space loss is the sum of different contributions such as attenuation due to atmospheric gases, diffraction fading due to obstruction or partial obstruction of the path, fading due to multipath and attenuation due to precipitation.

1.2 Statement of the Research Problem

The interaction between tropospheric factors and radio waves at frequencies above 30 MHz exposes the waves to important propagation characteristics which often degrade communication links especially at higher frequencies. The propagation of electromagnetic waves in the atmosphere (mainly the troposphere) is greatly affected by the composition of the atmosphere. Refractive bending causes extension of the radio horizon beyond the optical horizon, as well as reduction of the radio horizon. The refractivity gradient dN/dh, determines the refractivity condition of the atmosphere which may be normal, sub-refractive, super-refractive or ducting layer, each of which has important influence on propagation of Very High Frequency (VHF), Ultra High Frequency (UHF) and microwaves in the atmosphere. Sub-refractive conditions occur when radio waves are refracted less than normal or even, in extreme cases, curved upward from the Earth's surface. Sub-refraction occurs when the refractivity gradient is greater than −40 N-units/km, with waves that offer the smallest ranges and worst opportunity for distant detection. Super-refraction is experienced in the troposphere when the radio waves refract downwards at a rate greater than the standard value (-40 N-units/km) but less than the curvature of the earth. It extends the radio waves beyond the normal radio horizon of the transmitter; and may act like a waveguide which traps radio frequency (RF) wave. Ducting occurs when the refractivity gradient is less than -157 N-units/km. During this condition, radar microwaves may be trapped and can travel within the duct layers like in waveguide. This may lead to signal enhancement near and beyond radio horizon. Thus, good knowledge of radio refractivity as well as the diurnal and seasonal variability is particularly useful in planning terrestrial radio links. This research focuses on the effect of radio refractivity in parts of Northern Nigeria namely Bauchi, Kano and Yola state.

1.3 Justification for the Study

Radio signals can travel over vast distance. However, radio signals are affected by the medium in which they travel and the distances over which the signals propagate. In the lower atmosphere, the refractive index which is a function of some atmospheric parameters (pressure, temperature and humidity) is an important factor for predicting the performance of terrestrial radio links. Abnormal variations of these atmospheric parameters result to anomalous propagation such as sub-refraction, super-refraction and ducting. Therefore, this means that the signal propagating through the troposphere does not arrive at its destination with the expected amount of energy when these atmospheric conditions take certain values. Thus, the knowledge of refractivity is essential in order to design reliable and efficient radio communication. The study will provide an update and new information on N_s in Kano and in other parts of the study area.

1.4 Scope of the Study

This research work will provide necessary information and computations of radio refractivity and the atmospheric conditions of the study area using five-year (2012-2016) data of temperature, atmospheric pressure and relative humidity over Kano, Bauchi and Yola sourced from Nigeria Meteorological Agency (NIMet), Abuja and Centre for Atmospheric Research (CAR), Anyigba, which is an activity centre under the National Space Research and Development Agency (NASRDA).

1.5 Aim and Objectives of the Study

The aim of this research is to study radio refractivity over the Northern Nigerian cities of Bauchi, Kano and Yola.

The objectives of the research are to:

i. Compute the diurnal and seasonal variation of radio refractivity over the study area in Nigeria;
ii. Compute radio refractivity gradient and effective earth radius factor;
iii. Compare surface refractivity profiles in parts of the study area; and
iv. Determine the nature of field strength variability (FSV) in the study area.

1.6 Study Area

The study area are capital states in Northern parts of Nigeria. They are Bauchi, Kano and Yola.

1.6.1 Bauchi State

Bauchi state occupies a total land mass of 49,119 km^2 representing about 5.3 percent of Nigeria's total land mass and is located between latitudes 10.30° N and 9.84° E as shown in Figure 1.1. It is bordered by seven States, Kano and Jigawa to the North, Taraba and Plateau to the South, Gombe and Yobe to the East and Kaduna to the West. It is located on the Northern edge of the Jos Plateau, at an elevation of 616 m (Bauchi State, 2019).

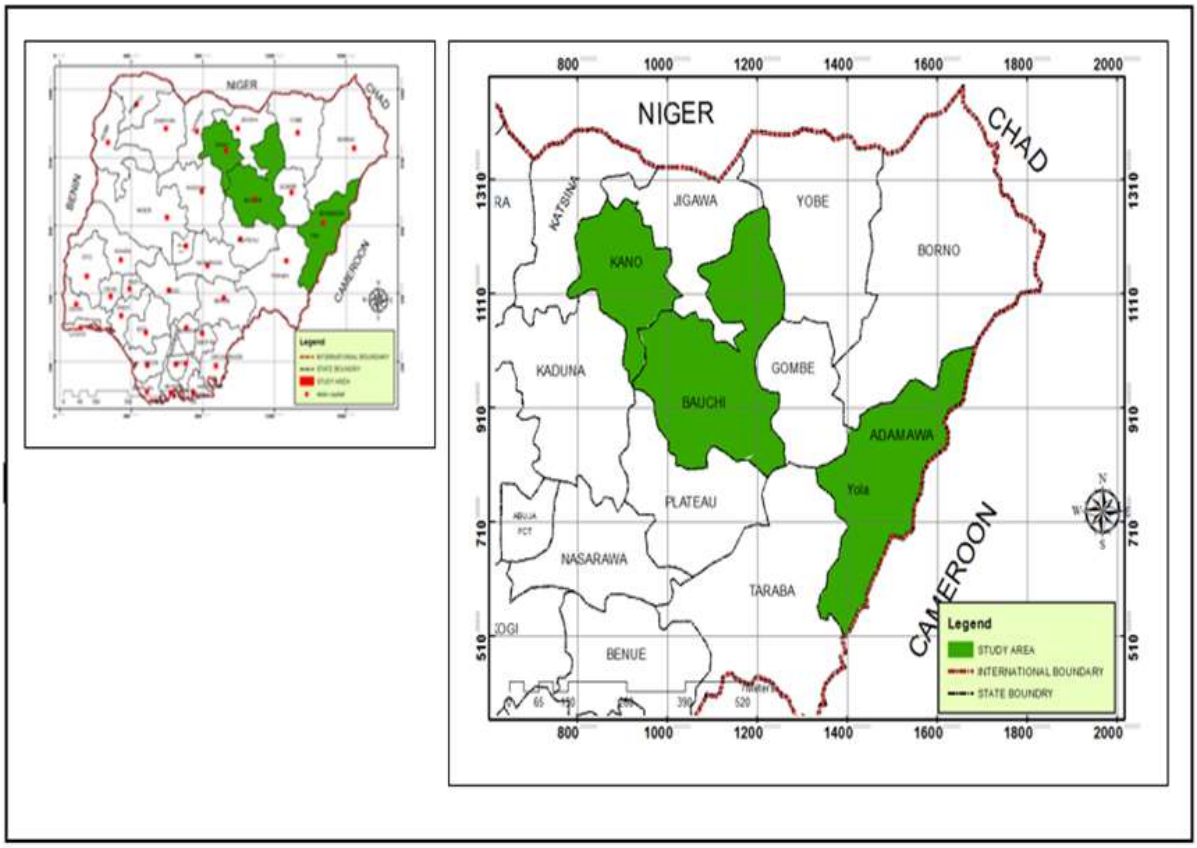

Figure 1.1: Showing positions of Bauchi, Kano and Adamawa State

Source : (Researchgate, 2019)

It is one of the states in the Northern part of Nigeria that covers two distinctive vegetation zones, namely, the Sudan savannah and the Sahel savannah. The vegetation types as described above are conditioned by the climatic factors which in turn determine the amount of rainfall received in the area. Consequently, rains start earlier in the Southern part of the state, where rain is heaviest and lasts longer. Here the rains start in April with the highest record amount of 1,300 millimetres per annum. In contrast, the Northern part of the state receives the rains late, usually around June or July, and records the highest amount of 700 millimetres per annum. The month with the highest rainfall is August, the rain falls for 21 days and typically aggregates up to 340 mm with a pressure

of 1012 hPa level rising or decreasing. In the same vein, the weather experienced in the South and the North varies considerably. While it is humidly hot during the early part of the rainy season in the South, the hot, dry and dusty weather lingers up North. Between the driest and wettest months, the difference in precipitation about 287 mm. Atmospheric pressure is normal at 1013 hPa. With an average high-temperature of 36.6℃ and average low-temperature of 22.3℃, April is the warmest month in Bauchi, the least humid month is February with an average relative humidity of 35 percent, while August is the most humid month with an average relative humidity of 94 percent (Bauchi State, 2019).

1.6.2 Kano State

Kano state is a state in North-West Nigeria. The capital of Kano state is Kano. It is situated in the Sahelian geographic region, South of the Sahara. Kano is the commercial nerve centre of Northern Nigeria and is the second largest city in Nigeria as shown in Figure 1.1. It is bordered by Katsina State to the North-West, Jigawa State to the North-East, Bauchi State to the South-East and Kaduna State to the South-West.

It is located between latitude 12.00°N and between longitude 8.59°E with an elevation of 481 m above sea level. The state features a tropical savanna climate. The city experiences an average of 980 mm of precipitation per year, the bulk of which falls from June through September. The month with the most rainfall is August, the rain falls for 14 days and have an aggregate of about 228 mm with atmospheric pressure of about 1012 hPa. Kano is typically very hot throughout the year, though from December through February, the city is noticeably cooler. April is the warmest month with an average high-temperature of 38.2℃ and an average low-temperature of 23.6℃. The average annual percentage of humidity is 51 percent. Night-time temperatures are cool during the

months of December, January and February, with average low temperatures of 11 °C to 15 °C (Kano State, 2019).

1.6.3 Yola State

Yola is the capital city and administrative centre of Adamawa State, Nigeria. It is located between latitude 9.20° N and between longitude 12.48° E and it is situated at an elevation of 162 m above sea level as shown in Figure 1.1. The climate is tropical in Yola. The rainy season has a great deal of rainfall, while the dry season has very little. The average annual temperature is 28 ^{o}C in Yola. In a year, the average rainfall is 933 mm. The driest month is January with 0 mm of precipitation. Most of the precipitation falls in August, averaging 211 mm. With an average of 32.1 ^{o}C, April is the warmest month. December is the coldest month with temperature averaging 25.9 ^{o}C. The average pressure is 1011 hPa (Yola, 2019).

CHAPTER TWO

LITERATURE REVIEW

2.1 The Atmosphere

The atmosphere is derived from the Greek word (*atmos*), meaning "vapour" and (*sphaira*) "ball" or "sphere" and is a set of layers of gases surrounding the planet or other material body that is held by gravity. The atmosphere of the earth is composed of Nitrogen (about 78 percent by volume) which is converted by bacteria and lightning to produce Ammonia, Oxygen (about 21 percent and mainly used for respiration), Argon (about 0.9 percent), Carbon-dioxide (about 0.04 percent) used by plants and algae for photosynthesis, and other gases in trace amounts (Earth's atmosphere composition, 2017).

2.2 Layers of the Atmosphere

The atmosphere is divided into 6 (six) distinct layers based on temperature distribution and content, these layers are troposphere, stratosphere, mesosphere, thermosphere, ionosphere and exosphere as shown in Figure 2.1.

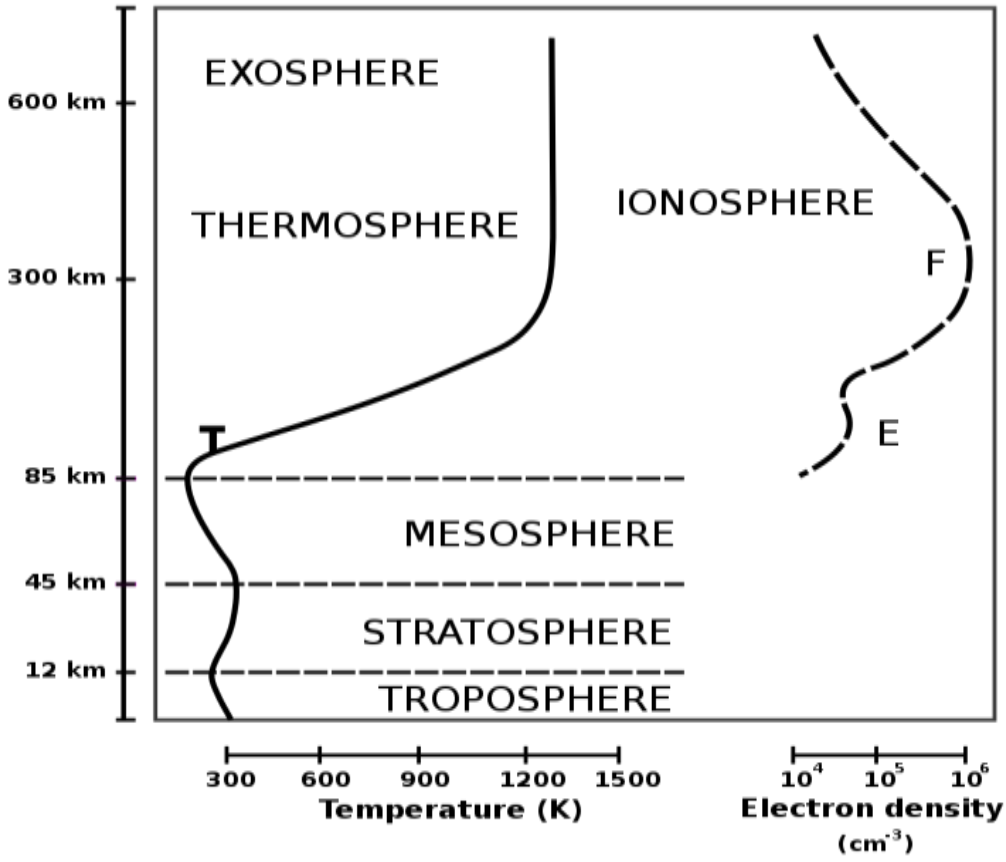

Figure 2.1: The Layers of the Earth's Atmosphere and Ionosphere

Source: (Ionosphere, 2019)

2.2.1 Troposphere

The troposphere is the lowest layer of the atmosphere. The troposphere extends from the surface of the earth to an altitude of approximately 9 km at the poles and 17 km at the equator. All weather conditions and clouds occur here. In this part of the atmosphere, the temperature gets colder as the distance above the earth increases, by about 6.5℃ per km. The actual change of temperature with height varies from day to day depending on the weather. The decrease in temperature with height is a result of decreasing pressure. The lowest part of the troposphere is called the planetary boundary layer. The top of the troposphere or interface between the troposphere and the

stratosphere is called the tropopause and is defined as the point at which the temperature in the atmosphere begins to increase with height. This is lowest at the poles, which is about 7-10 km above earth's surface (Layers of the atmosphere, 2020).

2.2.2 Stratosphere

This extends upwards from the tropopause to about 50 km. It contains much of ozone in the atmosphere. Ozone molecules in this layer absorb high-energy ultraviolet (UV) light from the sun, converting the UV energy into heat (Layers of the earth's atmosphere, 2015).

2.2.3 Mesosphere

Above the stratosphere is the mesosphere. It extends upward to a height of about 85 km above the atmosphere. Most meteors burn up in the mesosphere. In the mesosphere, temperatures decrease with height (grow colder as you rise up through the mesosphere), reaching a minimum of about -90℃ at the mesopause (Layers of the earth's atmosphere 2015).

2.2.4 Thermosphere

The layer of very rare air above the mesosphere is called the thermosphere. High-energy X-rays and Ultraviolet (UV) radiation from the sun are absorbed in the thermosphere, raising its temperature to hundreds or at times thousands of degrees. However, the air in this layer is so thin that one would feel freezing cold (Layers of the earth's atmosphere, 2015).

2.2.5 Ionosphere

The ionosphere is a region in parts of the mesosphere and thermosphere where high-energy radiation from the sun has knocked electrons loose from their parent atoms and molecules (Layers of the atmosphere, 2020).

2.3 Mode of Propagation of Electromagnetic Waves in the Atmosphere

- Line-of-sight propagation
- Ground wave propagation
- Skywave propagation

Line-of-sight propagation simply means the transfer of radio waves from a transmitting antenna to a receiving antenna. It can also be defined as a propagation which travels a minimum distance, as it implies, it can be seen clearly. Line-of-sight transmission is used for short range transmission such as radar, cellphones, walkie-talkie, televisions broadcasting, FM radio and wireless networks. It is the only propagation which uses infrared or microwave transmissions (What are the methods of propagation, 2019).

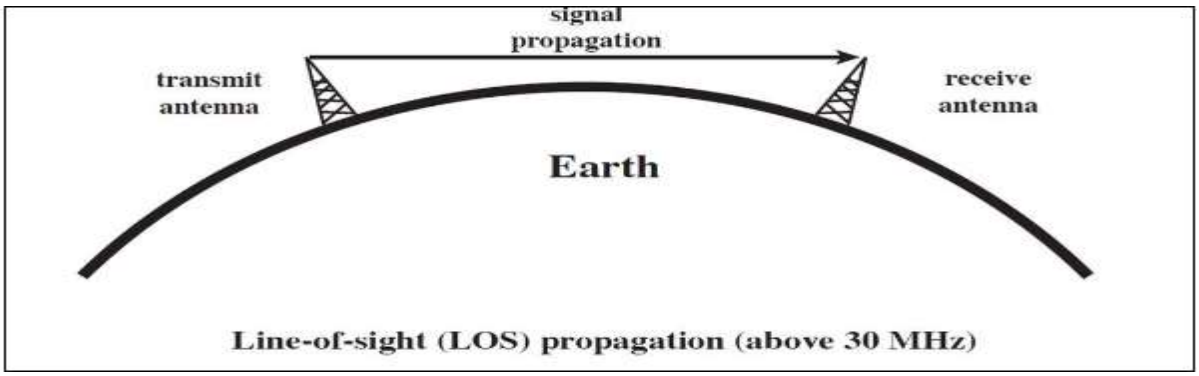

Figure 2.2: Line-of-sight Propagation

Source: (Wave propagation, 2019)

Due to the distance of the visual horizon on the earth's surface, line-of-sight transmission is limited and depends on the height of the transmitting antenna and the height of the receiving antennas. Also, line-of-sight propagation will not be smooth if there is any obstacle in its transmission path.

Ground wave propagation can be referred to as direct wave or reflected wave. At lower frequency in the Medium Frequency (MF), Low Frequency (LF), and Very Low Frequency (VLF) bands,

radio waves bend over obstacles due to diffraction and travel beyond the horizon as surface waves, which follow the contour of the earth. These waves are called Ground waves (see Figure 2.3).

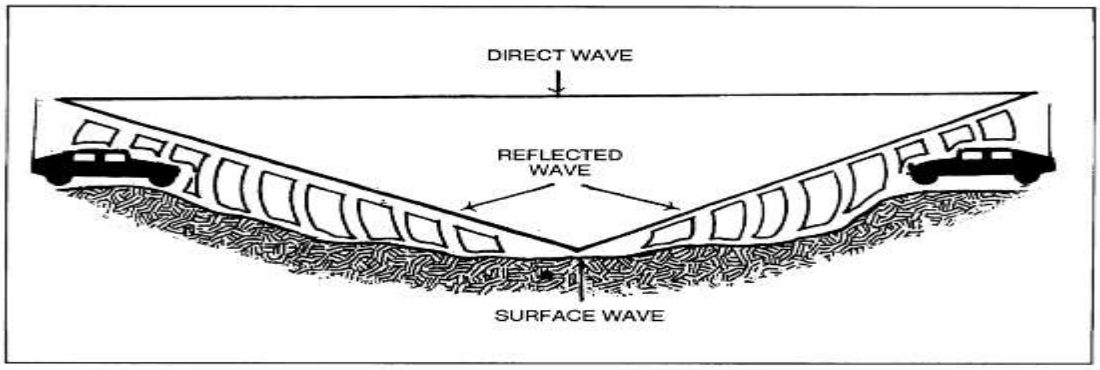

Figure D-2. Components of ground wave.

Figure 2.3: Ground Wave Propagation

Source: (Wave propagation, 2019)

The above figure depicts ground wave propagation. The direct wave and reflected wave contribute to the signal at the receiver station. When the wave finally reaches the receiver, the lags are cancelled out. In addition, the signal is filtered to avoid distortion and amplified for clear output, as the frequency, the attenuation with distance reduces so Very Low Frequency (VLF) and Extremely Low Frequency (ELF) can be used to communicate worldwide because they can penetrate significant distances through water and earth. These frequencies are used for mine and military communications (Wave propagation, 2019).

Skywave propagation are transmission projected into the sky and it is reflected back to the earth. These transmission covers long range distance. The waves are transmitted from the transmitting antenna into the ionosphere, the ionosphere reflects the waves back to the receiving antenna, that is, earth (see Figure 2.4).

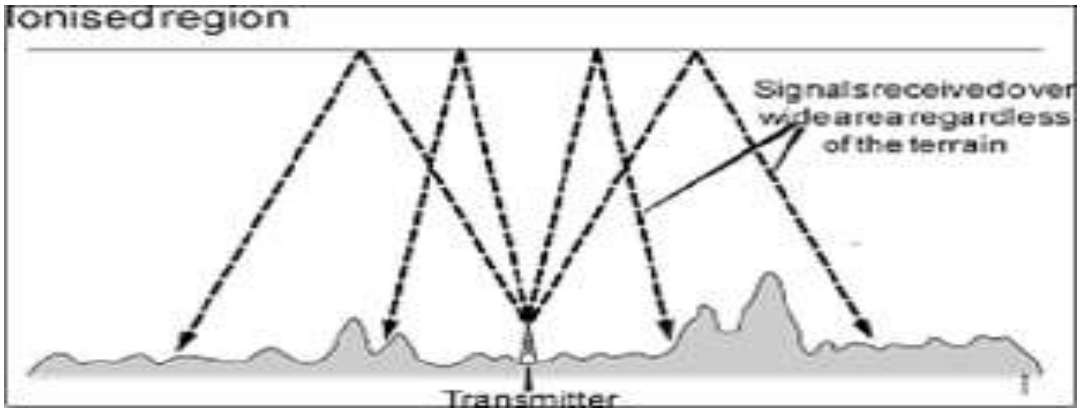

Figure 2.4: Skywave Propagation

Source: (Wave propagation, 2019)

The ionosphere is the ionised layer around the earth's atmosphere which is suitable for propagation. Skywave propagation is used by amateur radio operators to talk to other countries and shortwave broadcasting stations. It is more reliable at night and during winter (when the ionizing effect of the sun rays is lowest). It uses medium and short-wave frequencies i.e. Medium Frequency (MF) and High Frequency (HF) bands (Wave propagation, 2019).

2.4 Radio Wave Frequency and their Modes of Propagation

The radio spectrum is divided into frequency bands with conventional names and wavelengths designated by ITU (International Telecommunications Union). Table 2.1 shows radio frequency bands, wavelength, frequency and their modes of propagation.

Table 2.1: Radio Frequency Bands

BAND	FREQUENCY	WAVELENGTH	PROPAGATION MODE
Extremely Low Frequency (ELF)	3-30 Hz	100,000-10,000 km	Guided between the Earth and the D layer of the ionosphere.
Super Low Frequency (SLF)	30-300 Hz	10,000-1,000 km	Guided between the Earth and the ionosphere.
Ultra-Low Frequency (ULF)	0.3-3 kHz (300-3,000 Hz)	1,000-100 km	Guided between the Earth and the ionosphere.
Very Low Frequency (VLF)	3-30 kHz (3,000-30,000 Hz)	100-10 km	Guided between the Earth and the ionosphere.
Low Frequency (LF)	30-300 kHz (30,000-300,000 Hz)	10-1 km	Guided between the Earth and the ionosphere. Ground waves.
Medium Frequency (MF)	300-3,000 kHz (3,000,000)	1000-100 m	Ground waves. E, F layer ionospheric refraction at night, when D layer absorption weakens.
High Frequency (HF) short wave	3-30 MHz (3,000,000-30,000,000Hz)	100-10 m	E layer ionospheric refraction. F1, F2 layer ionospheric refraction.
Very High Frequency (VHF)	30-300 MHz (30,000,000-300,000,000 Hz)	10-1 m	Line-of-sight propagation. Infrequent E ionospheric (E_s) refraction. Uncommonly F2 layer ionospheric refraction during high sunspot activity up to 50MHz and rarely to 80MHz. Sometimes tropospheric ducting or meteor shower.
Ultra-High Frequency (UHF)	300-3000 MHz (300,000,000-3,000,000,000 Hz)	100-10 cm	Line-of-sight propagation. Sometimes tropospheric ducting.
Super High Frequency (SHF)	3-30 GHz (3,000,000,000-30,000,000,000 Hz)	10-1 cm	Line-of-sight propagation. Sometimes rain scatter.
Extremely High Frequency (EHF)	30-300GHz (30,000,000,000-300,000,000,000 Hz)	10-1 mm	Line-of-sight propagation, limited by atmospheric absorption to a few kilometres.
Tremendously High Frequency (THF)	0.3-3THz (300,000,000,000-3,000,000,000,000 Hz)	1-0.01 mm	Line-of-sight propagation.

Source: (Seybold, 2005)

2.5 Refraction

Refraction is the change in the direction of a wave passing from one medium to another. Refraction of waves is the bending of the path of the wave accompanied by a change in speed and wavelengths. The atmospheric radio refractivity is an important factor in the propagation of radio waves in VHF and UHF bands. The path and general characteristics of the signals are very much tied to the refractive conditions of the troposphere (Oyedum and Gambo, 1994). Using Snell's law, a radio ray projected into the atmosphere will have to travel from a denser to rarer medium and will refract downwards towards the surface of the earth. The curvature of the ray, however, will still be less than the earth's curvature. The gradient of refractivity in this case generally varies from 0 to –79 N-units/km. When the refractivity gradient varies from –79 to –157 N-units/km, a super refractive condition is said to prevail in the troposphere and the ray will refract downwards at a rate greater than standard but still less than the curvature of the earth. A refractivity gradient that is even less than –157 N-units/km will result in a ray that refracts towards the earth's surface with a curvature that exceeds the curvature of the earth. This situation is referred to as trapping and is of particular importance in the context of evaporation ducts. Finally, if the refractivity gradient is greater than 0 N units/km, a sub-refractive condition exists and a radio ray will now refract upwards, away from the surface of the earth.

Depending on the existing conditions in the troposphere, a radio wave will undergo any of the types of refraction as shown in Table 2.2 namely sub-refraction, standard refraction, super-refraction and ducting are. In terms of refractive index, whenever the vertical refractivity gradient $^{dN}/_{dh}$ of the atmosphere is less than the standard refractivity gradient of −40 N-units/km the radio ray will undergo super refraction. On the other hand, the radio ray will be sub-refracted whenever

$dN/_{dh}$ is greater than −40 N-units/km. If $dN/_{dh}$ in a layer of the atmosphere is equal to −157 N-units/km, the curvature of the path is equal to that of the earth. On occasions when meteorological conditions are such that the vertical gradient is less than −157 N-units/km, trapping or ducting of the rays may occur depending on the wavelength and duct thickness (Barclay, 2003). A consequence of super-refraction and ducting is the extension of the radio range, which sometimes leads to radio interference between neighboring transmission links. On the other hand, sub-refraction reduces radio horizon.

Table 2.2: **Types of Refraction with corresponding Refractivity Gradient and k Values**

Types of Refraction	$dN/_{dh}$ **Refractivity Gradient (N-units/km)**	**K values**
Homogeneous	0	1
Adiabatic	-23	1.2
Standard	-40	4/3
Sub-refraction	>-40	<4/3
Extreme Sub-refractive	>0	<1
Super-refraction	<-40	>4/3
Ducting Threshold	-157	∞
Ducting	<-157	∞

Source: (Monebhurrun, 2021)

For an ideal condition of the atmosphere, the atmosphere is uniformly stratified, and the vertical gradient of the refractive index is assumed constant and defined by (Fashade *et al.*, 2019):

$$k = \frac{1}{1+R\frac{dn}{dh}} = \frac{1}{1+R\frac{dN}{dh}10^{-6}} = \frac{10^6}{R\frac{dM}{dh}} \quad (2.1)$$

where $k =$ effective earth-radius factor, R is radius of the earth (in kilometres), $M$is refractive modulus (for air) and $N$is radio refractivity (Fashade *et al.*, 2019).

Figure 2.5 illustrates the four refractive conditions discussed above: sub-refraction, super-refraction, standard refraction and ducting.

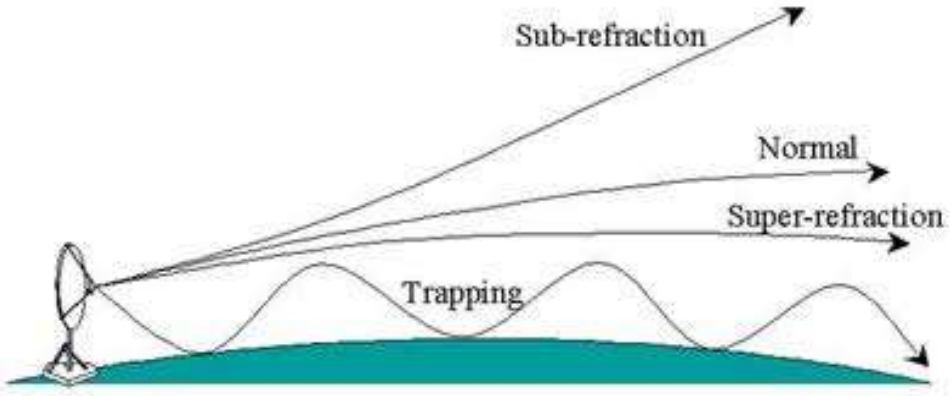

Figure 2.5: Refractive Conditions in the Atmosphere

Source: (Mahdi *et al*., 2017).

2.6 Theory of Refraction

As a ray moves from one layer of the atmosphere to another, it bends, that is, it is refracted. If it moves from a medium with refractive index n_1 to one with refractive index n_2, with an incidence angle to the surface normal of θ_1, the refraction angle θ_2 can be calculated from Snell's law as shown in Figure 2.6. When light enters a material with higher refractive index, the angle of refraction will be smaller than the angle of incidence and the light will be refracted towards the normal of the surface. The higher the refractive index, the closer to the normal direction the light will travel. When passing into a medium with lower refractive index, the light will instead be refracted away from the normal, towards the surface according to Snell's law (Byjus, 2020):

$$n_1 sin(\theta_1) = n_2 sin(\theta_2) \quad (2.2)$$

where n_1: refractive index of incident ray in medium 1, n_2: refractive index of refracted ray in medium 2, θ_1: Incident angle in medium 1 and θ_2: refracted angle in medium 2.

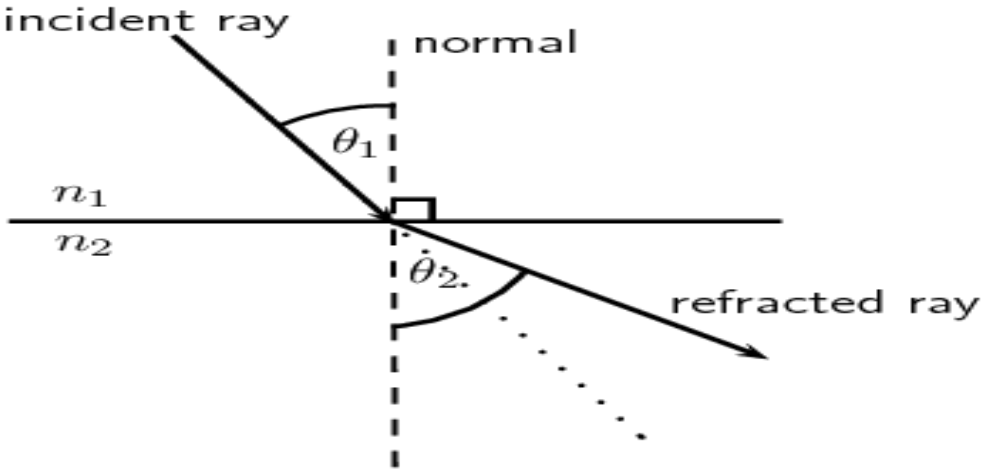

Figure 2.6: Snell's Law

Source: (Byjus, 2020)

2.7 Radio Refractivity

The radio refractive index, *n*, of the troposphere deviates slightly from unity due to the unity of the constituent molecules by the incident electromagnetic field, and the quantum mechanical resonances at certain frequency bands, while molecular is independent of frequency up to millimeter waves, molecular resonance is totally frequency dependent, and *n* tends to be dispersive above 50 GHz (Bean and Dutton, 1968).

Atmospheric refractivity is dependent on physical parameters of air such as pressure, temperature and water content. It varies in space and time due to physical processes in the atmosphere that are often difficult to describe in a deterministic way and have to be, to some extent, considered as random with its probabilistic characteristics (Martin and Vaclav, 2011). The refractivity, N of the earth's atmosphere is the difference between refractive index of air scaled up to a million and may

be calculated from observations of pressure, temperature and relative humidity at the surface of the earth using the relation in equation 2.3. The surface refractivity gradient is the gradient of refractive index between the surface and a given altitude, such as between the surface and 1000 m (ITU-R, 2019). In order to have an easier number to handle, the radio refractivity, N can be written as (Hall, 1980):

$$N = (n - 1) \times 10^6 \tag{2.3}$$

where *n* is the refractive index of air

For frequencies up to about 30 GHz, the radio refractive index of clear air is given by the formula (Smith and Weintraub, 1953):

$$N = \frac{77.6}{T}\left(P + 4810\frac{e}{T}\right) \tag{2.4}$$

Note: $1mb = 1hPa$

Equation 2.4 can also be rewritten as:

$$77.6\frac{P}{T} + 3.732 \times 10^5 \frac{e}{T^2} \tag{2.5}$$

where P is pressure (in millibars or hPa), T is temperature (in Kelvins) and e is the water vapour pressure(mb).

2.8 Atmospheric Parameters for Surface Radio Refractivity

There are four meteorological parameters for radio refractivity namely atmospheric pressure, dew point, relative humidity and temperature

2.8.1 Atmospheric pressure

Atmospheric pressure, also known as barometric pressure is the pressure within the atmosphere of the earth. The standard atmosphere (symbol: atm) is a unit of pressure defined as 101,325 Pa (1,013.25 hPa), which is equivalent to 760 mm Hg. The atm unit is roughly equivalent to the mean sea-level atmospheric pressure on earth, that is, the earth's atmospheric pressure at sea level is approximately 1 atm. Pressure measures force per unit area, with SI unit of Pascals (1 pascal = 1 newton per square metre, 1 N/m^2). In aviation, weather reports (METAR), QNH (Question Nill Height) is transmitted around the world in millibars or hectopascals (1 hectopascal = 1 millibar). It is directly proportional to the mass of air over that location. The average pressure at mean sea-level (MSL) in the International Standard Atmosphere (ISA) is 1013.25 hPa, or 1 atmosphere (atm). Pressure (p), mass (m), and the acceleration due to gravity (g), are related by (Jacob,1999).

$$p = {F}/{A} = {(m \times g)}/{A} \tag{2.6}$$

where A is surface area. At low altitudes above sea level, the pressure decreases by about 1.2 kPa (12 hPa) for every 100 metres. According to the International Civil Aviation Organisation (ICAO, 1993) for higher altitudes within the troposphere, the following equation (the barometric formula) relates atmospheric pressure, *p*, to altitude *h*:

$$p = p_0 . \left(1 - \frac{L.h}{T_0}\right)^{\frac{g.M}{R_0.L}} \tag{2.7}$$

$$p = p_0 . \left(1 - \frac{g.h}{c_p T_0}\right)^{\frac{c_p.M}{R_0}} \approx p_{0\ .exp\left(-\frac{g.h.M}{T_0.R_0}\right)} \tag{2.8}$$

where the constant parameters are as described in Table 2.2:

Table 2.3: The Barometric Formula Parameters

Parameter	Description	Value
p_0	Sea level standard atmospheric pressure	101325 Pa
L	Temperature lapse rate, = g/c_p for dry air	~ 0.00976 K/m
c_p	Constant-pressure specific heat	1004.68506 J/(kg·K)
T_0	Sea level standard temperature	288.16 K
G	Earth-surface gravitational acceleration	9.80665 m/s^2
M	Molar mass of dry air	0.02896968 kg/mol
R_0	Universal gas constant	8.314462618 J/(mol·K)

Source: (PSAS, 2011)

2.8.2 Dewpoint

The dew point is the temperature to which air must be cooled to become saturated with water vapour. When cooled further, the airborne water vapour will condense to form liquid water (dew). When air cools to its dew point through contact with a surface that is colder than the air, water will condense on the surface. When the temperature is below the freezing point of water, the dew point is called the frost point, as frost is formed via deposition rather than condensation to form dew. Devices called hygrometers are used to measure dew point over a wide range of temperatures. These devices consist of a polished metal mirror which is cooled as air is passed over it. The temperature at which dew forms is, by definition, the dew point. Manual devices of this sort can be used to calibrate other types of humidity sensors, and automatic sensors may be used in a control loop with a humidifier or dehumidifier to control the dew point of the air in a building or in a smaller space for a manufacturing process. There is also a very simple approximation that allows

conversion between the dew point, temperature, and relative humidity. This approach is accurate to within about $\pm$ 1℃ as long as the relative humidity is above 50 percent (Lawrence, 2005):

$$T_{dp} \approx T - \frac{100-RH}{5} \tag{2.9}$$

$$RH \approx 100 - 5(T - T_{dp}) \tag{2.10}$$

According to Lawrence (2005) this can be expressed as a simple rule of thumb which states that "for every 1°C difference in the dew point and dry bulb temperatures, the relative humidity decreases by 5%, starting with RH = 100% when the dew point equals the dry bulb temperature".

2.8.3 Relative humidity

Relative humidity (RH) is the ratio of the partial pressure of water vapour to the equilibrium vapour pressure of water at a given temperature. Relative humidity depends on temperature and the pressure of the system of interest. The same amount of water vapour results in higher relative humidity in cool air than warm air. The relative humidity of air is a function of both its water content and temperature and it is normally expressed as percentage (Wyer,1906).The relative humidity ($\emptyset$) or RH of an air–water mixture is defined as the ratio of the partial pressure ρH_2O of water vapour in the mixture to the equilibrium vapour pressure $\rho^* H_2O$ of water over a flat surface of pure water at a given temperature (Lide, 2005).

$$\emptyset = \frac{\rho H_2O}{\rho^* H_2O} \tag{2.11}$$

Relative humidity is normally expressed as a percentage, a higher percentage means that the air–water mixture is more humid. At 100 percent relative humidity, the air is saturated and is at its dew point. A hygrometer is a device used for measuring the humidity of air. The humidity of air and

water vapour mixture is determined through the use of psychrometric charts if both the dry bulb temperature (T_d) and the wet bulb temperature (T_w) of the mixture are known. These quantities are readily estimated by using a sling psychrometer. There are several empirical formulas that can be used to estimate the equilibrium vapour pressure of water vapour as a function of temperature. The Antoine equation is among the least complex of these, having only three parameters (*A*, *B*, and *C*). Other formulas, such as the Goff-Gratch equation and the Magnus-Tetens approximation, are more complicated but yield better accuracy. The Arden Buck equation is commonly encountered in the literature regarding this topic (Buck, 1981).

$$e^*_w = (1.0007 + 3.46 \times 10^{-6} P) \times 6.11 \qquad (2.12)$$

where T is the dry-bulb temperature expressed in degrees Celsius (°C), P is the absolute pressure expressed in millibars, and e_w is the equilibrium vapour pressure expressed in millibars. Buck (1981) has reported that the maximal relative error is less than 0.20% between −20 °C and +50 °C when this particular form of the generalized formula is used to estimate the equilibrium vapour pressure of water.

2.8.4 Temperature

Temperature is a physical property of matter that quantitatively expresses hot and cold. It is the manifestation of thermal energy present in all matter which is the source of the occurrence of heat, a flow of energy when a body is in contact with another that is colder. Atmospheric temperature is a measure of temperature at different levels of the earth's atmosphere. It is governed by many factors including incoming solar radiation, humidity and altitude. When discussing surface air temperature, the annual atmospheric temperature range at any geographical location depends

largely upon the type of biome as measured by the K*ö*ppen climate classification. Temperature is measured with a thermometer. Thermometers are calibrated in various temperature scales that historically have used various reference points and thermometric substances for definition. The most common scales are the Celsius scale (formerly called centigrade, denoted °C), the Fahrenheit scale (denoted °F), and the Kelvin scale (denoted K), the last of which is predominantly used for scientific purposes by convention of the International System of Units (SI). The lowest theoretical temperature is absolute zero at which no more thermal energy can be extracted from a body. Experimentally, it can only be approached very closely but not reached which is recognized in the third law of thermodynamics (Bolton, 1980).

2.9 Maxwell's Equations

Maxwell's equations are a set of coupled partial differential equations that, together with the Lorentz force law, form the foundation of classical electromagnetism, classical optics, and electric circuits. The equations provide a mathematical model for electric, optical, and radio technologies, such as power generation, electric motors, wireless communication, lenses, radar. They describe how electric and magnetic fields are generated by charges, currents, and changes of the fields. The equations are named after the physicist and mathematician James Clerk Maxwell, who, in 1861 and 1862, published an early form of the equations that included the Lorentz force law. Maxwell first used the equations to propose that light is an electromagnetic phenomenon. An important consequence of Maxwell's equations is that they demonstrate how fluctuating electric and magnetic fields propagate at a constant speed, *c*, in a vacuum. Known as electromagnetic radiation, these waves may occur at various wavelengths to produce a spectrum of light from radio waves to

gamma rays. Maxwell's equations comprise of four (4) laws namely: Gauss's law for electricity, Gauss's law for magnetism, Faraday's law of induction and Ampere's law (Hampshire, 2018).

2.9.1 Differential Form of Maxwell's Equation

$$\vec{\nabla} \cdot \vec{D} = \rho \ (\ Gauss's\ Law\ for\ electricity) \tag{2.13}$$

$$\vec{\nabla} \cdot \vec{B} = 0 \ (Gauss's\ Law\ for\ Magnetism) \tag{2.14}$$

$$\vec{\nabla} \times \vec{E} = \frac{\partial \vec{B}}{\partial t} (Faraday's\ Law\ of\ Induction) \tag{2.15}$$

$$\vec{\nabla} \times \vec{H} = \vec{J} + \frac{\partial \vec{D}}{\partial t} (Ampere - Maxwell's\ Law) \tag{2.16}$$

Together with the Lorentz force as shown in equation 2.17, these equations form the basis of the classic electromagnetism.

$$\vec{F} = q\left(\vec{E} + \vec{v} \times \vec{B}\right) \tag{2.17}$$

D= electric flux density/displacement field (C/m^2)

B = magnetic flux density (Tesla)

E= electric field intensity (V/m)

H = magnetic field intensity (A/m)

ρ= electric charge density (C/m^3)

J = electric current density (A/m^2)

F= force (N)

q= charge (C)

2.10 Related Works on Radio Refractivity

Adediji and Ajewole (2008) computed the vertical profile of radio refractivity gradient in Akure South-West Nigeria. In this work, measurements of atmospheric pressure, temperature and relative humidity were made in Akure (7.15^o N, 5.12^oE), South Western Nigeria. Wireless weather stations (Integrated Sensor Suite, ISS) were positioned at five (5) different height levels beginning from the ground surface and at intervals of 50 m from the ground to a height of 200 m (0, 50, 100, 150 and 200 m) on a 220 m Nigeria Television Authority (NTA) tower at Iju in Akure North local government area of Ondo state. The measurement of the atmospheric variables was made every 30 minutes daily. The study utilized the data for the first year of measurement (January–December 2007) to compute the radio refractivity and its refractivity gradient in Akure. From these parameters, the vertical distributions of radio refractivity are then determined. The results obtained show that the propagation conditions have varying degree of occurrence with sub-refractive conditions observed to be prevalent between January–July while super-refraction and ducting were observed mostly between August–December.

Adedayo (2016) deduced the statistical analysis of the effects of relative humidity and temperature on radio refractivity over Nigeria using satellite data. Meteorological data from the department of Satellite Application Facility on Climate Monitoring (CM-SAF), DWD Germany were used to study and investigate the effect of relative humidity and temperature on refractivity in twenty-six locations grouped into four climatic regions aloft Nigeria (Coastal, Guinea savannah, Midland and

sub-Sahelian regions). The four years data collected ranged from 2004 to 2007 and was evaluated on their linear variation of refractivity on both temperature and relative humidity at different atmospheric levels. The coefficient of determination (CD) was also determined for each relation. The results obtained established the seasonal variation of temperature and relative humidity with refractivity across the regions especially at low and mid-level. The coefficient of determination at both regions are high for the variations measured against relative humidity and refractivity, while that of temperature and refractivity is low. This affirms that changes in relative humidity influence refractivity more than temperature at lower and middle levels. Analysis of refractivity, relative humidity and temperature aloft Nigeria revealed that the variation of refractivity vary seasonally from one region to other. Levels of temperature, relative humidity and refractivity were analysed using techniques applied by Balogun and Adedokun (1986), Adeyemi (2004) and Adeyemi and Emmanuel (2011). The profiles of temperature, relative humidity and refractivity were grouped into low level, TL, R_hL, NL (surface – 925 hPa); mid-level Tm, R_hm, Nm (775 – 600 mb) and upper level Tu, R_hu, Nu (400 – 250 mb). At low level, variation of NL and R_hL follow similar pattern which is high during the rainy months and low during the dry months while the case of temperature is a reverse. Influence of R_hL and TL over NL is noticeable. In addition, the following trends were also discovered from the study:

a) At low level, temperature increases northward and is much higher in the dry months than in rainy season. At the upper level, the variation of T or N does not have a particular pattern as it oscillates up and down. However, R_h is low in the dry season and rises in the rainy season. It is also observed that T, R_h and N decrease with atmospheric level.
b) At coastal and guinea savannah regions, higher and almost uniform values of relative humidity and refractivity parameters are observed throughout the year. Mean values of R_h

range between 52 percent and 76 percent at coastal region, 47 percent and 74 percent in the guinea savannah region. Mean values of N range between 323 and 334 N-units in coastal and between 312 and 336 N-units at guinea savannah.

c) In the case of midland and sub-Sahelian regions, R_h and N parameter values during the dry season are quite lower than those of rainy season. A similar situation was noticed at mid-level.

d) The distinction observed between the southern and the northern regions in relative humidity and refractivity may be attributed to the fact that the precipitation climatology of the two regions differ appreciably (Balogun, 1981).

From the statistics and linear regression and analysis of variance (ANOVA), poor correlation between N and T shows that linear regression cannot be used to predict the dependent parameter. In the case of N and R_h where good correlation exists, linear regression can be used to predict the dependent parameter. This shows that variability of N is majorly anchored on R_h parameter.

Ayantunji *et al.* (2011) determined the diurnal and seasonal variation of surface refractivity over Nigeria using four years meteorological data from eight locations (Nsukka, Akure, Jos, Port-Harcourt, Makurdi, Minna, Sokoto and Lagos) to cover all the climatic regions in Nigeria. From the work, the authors deduced that:

a) Refractivity value over Nigeria increases from about 270 N-units in the North to about 390 N-units in the South. The variation range of refractivity from Northern Nigeria to Southern Nigeria has a maximum range of about 120 N-units while the seasonal variation over the North has a maximum range of 90 N-units at Sokoto, while the maximum difference in the South is 65 N-units at Akure.

b) The diurnal refractivity variation was caused majorly by the dry term in the rainy season, while the wet term is the major cause of refractivity variation in dry season except Sokoto and Jos.

c) The surface refractivity generally has higher values during rainy season than dry season at all locations studied.

Estimation of radio refractivity is critical in the planning and design of radio links/systems for the purpose of achieving optimal performance. Akpootu *et al*. (2017) investigated the tropospheric radio refractivity over Ikeja, Lagos State, South Western Nigeria (Latitude 6.58^{o} N, Longitude 3.33^{o} E and altitude of 40 m above sea level) and the sensitivity of radio refractivity due to meteorological parameters of monthly average daily atmospheric pressure, relative humidity and temperature for a period of 12 years. The maximum average value of radio refractivity of 389.45 N-units and minimum average value of 373.04 N-units occurred during the rainy and dry seasons in the months of April and January respectively. The average refractivity gradient computed for the study area under investigation was −44.32 N-units/km while the average effective earth radius (k – factor) was 1.39 which correspond to conditions of super-refraction.

Lane and Bean (1963) obtained correlation coefficient of 0.70 between VHF field strength and surface refractivity, N_s and 0.71 between VHF field strength and ΔN. Other parameters also proposed for predicting or interpreting radio data include the equivalent gradient G_e (Misme, 1960), and the potential refractive index K (Flavell and Lane, 1962), while Saxton and Schmitt (1963) highlighted the relative merits of the parameters. However, N_s is commonly used because of the relative ease in obtaining the related surface parameters of temperature, pressure

and relative humidity from many widely separated stations. Bean and Thayer (1963) showed that elevation angle errors and range errors can also be predicted from N_s values. Earlier efforts in this regard with respect to Nigerian stations could not explore the diurnal trend due to paucity of data. Owolabi and Williams (1970) showed that N_s in Minna has an annual range of 300-375 N-units while the seasonal trend showed that N_s rises from February to April, is steady between April and September and decreases from October to a minimum in February.

The study by Kolawole (1980) revealed that reduced-to-sea-level surface refractivity N_0 in Nigeria varies from about 390 in the coastal areas in the South to about 280 in the Northern parts of the country. This agrees with Adebanjo (1977) but slightly differs from Owolabi and Williams (1970) due to the elevation dependence of N_s. Oyedum and Gambo (1994) obtained similar results and a correlation coefficient of 0.73 between N_s and trans-horizon VHF field strength values in Northern Nigeria. Oyedum (2005) showed that based on N_s variability, substantial climate-related differences exist between the seasonal variability of VHF field strength and radio horizon distance in two Nigerian stations of Lagos (6.27^o N, 5.12^o E) on the Atlantic coast and Kano (12.00^o N, 8.31^o E) in sub-Sahara Northern Nigeria. Oyedum *et al.* (2010) showed that reduced-to-sea-level refractivity in Minna (9.36^o N, 6.33^o E) has considerable diurnal and seasonal tendencies: Maximum values occur in the night while minimum values occur towards local evening; and a seasonal trend of higher values in rainy season and lower values in dry season.

Jidong *et al.* (2008) reported that during warm season, radio refractivity gradient is more sensitive to moisture gradient in some selected locations in USA. They concluded that moisture has a more significant influence on the radar ray path calculation than temperature. Some other

researchers worked on refractivity variation based on few available radiosonde stations data in Nigeria (Adeyemi, 2004; Willoughby *et al*., 2002; Kolawole and Owonubi, 1982) and few experimental sites where sensors were mounted on a radio transmitter to access atmospheric data (Adediji and Ajewole, 2008). Their results show that refractivity values were normally high during the rainy season and low in the dry season.

CHAPTER THREE

MATERIALS AND METHODS

3.1 Data Acquisition

The data used for this work were collected from two sources. Five-year (2012-2016) atmospheric variables (pressure, relative humidity and temperature) were obtained from the Centre for Atmospheric Research, Anyigba, an outfit of National Space Research and Development Agency (CAR-NASRDA) for Bauchi and Yola. Each location is equipped with wireless weather equipment which is part of the Tropospheric Data Acquisition Network (TRODAN) of CAR-NASRDA.

The second data was sourced from the upper air station of Nigerian Meteorological Agency (NIMet), Abuja. A set of radiosonde weather data over Kano station was collected for a period of five years (2012-2016) where a balloon ascent was launched at 12:00 Local time daily. The measurements period covered both the dry and wet seasons. The dry season months start from November to March while the wet season months start from April to October annually.

3.2 Techniques of Data Processing

The equations used for this work are the computations of radio refractive index and refractivity, modified refractivity, radio refractivity gradient, k-factor and field strength variability.

3.2.1 Refractive index and refractivity

It is more suitable to define variations of refractive index, *n*, in terms of a parameter called refractivity, N, which is defined as the degree of deviation of atmospheric refractive index, *n*, of air from unity scaled-up in parts per million as:

So that

$$N = (n - 1 \times 10^6) \tag{3.1}$$

$$n = 1 + \mathrm{N} \times 10^{-6} \tag{3.2}$$

Thus, N is measured in N-units and is a dimensionless quantity. ITU-R P.453-11 (2015) expressed radio refractivity, N, as:

$$N = 77.6\frac{P_d}{T} + 72\frac{e}{T} + 3.75 \times 10^5 \frac{e}{T^2} \tag{3.3}$$

the "dry term" of radio refractivity, N_{dry} is expressed by:

$$N_{dry} = 77.6\frac{P_d}{T} \tag{3.4}$$

and the "wet term" of radio refractivity, N_{wet} is expressed as:

$$N_{wet} = 72\frac{e}{T} + 3.75 \times 10^5 \frac{e}{T^2} \tag{3.5}$$

where P_d is dry atmospheric pressure (measured in hPa), T is absolute temperature (in Kelvin), e is water vapour pressure (in mb) and P is the total atmospheric pressure (in hPa).

The dry term is proportional to pressure, P, and therefore, related to the air density. The wet term is proportional to vapor pressure and dominated by polar water contents in the troposphere.

Also,

$$P = P_d + e \tag{3.6}$$

Therefore, equation (3.3) can be rewritten as:

$$N = \frac{P}{T} - 5.6\frac{e}{T} + 3.75 \times 10^5 \frac{e}{T^2} \tag{3.7}$$

(since $P_d = P - e$)

Equation (3.7) with reduced precision can be rounded off to:

$$N = \frac{77.6}{T}\left(P + 4810\frac{e}{T}\right) \tag{3.8}$$

The relationship between water vapour pressure, e (hPa) and relative humidity (%), H can be expressed as:

$$e = \frac{He_s}{100} \tag{3.9}$$

where

$$e_s = 6.11exp((19.7t)/(t + 273)) \tag{3.10}$$

and t is the temperature (in °C), while e_s is saturation vapour pressure (in hPa)

3.2.2 Modified refractivity

Modified radio refractivity is a dimensionless quantity and it is related to radio refractivity by:

$$M = N + (0.157 \times h) \tag{3.11}$$

where N is radio refractivity, M is the modified refractivity and h is the height in metres above sea level (Igwe *et al*. 2009).

3.2.3 Computation of refractivity gradient and k-factor

Change in radio refractivity, $\left(\frac{dN}{dh}\right)$ was computed using (Igwe *et al.* (2018):

$$\left(\frac{dN}{dh}\right) = \frac{N_1 - N_s}{h_{1-h_s}} \tag{3.12}$$

where N_1 is radio refractivity at a height of 1 km above earth's surface, N_s is surface refractivity, $h_1$is height at 1 km, h_s is surface height above sea level and $\frac{dN}{dh}$ is the refractivity gradient.

k- factor is given as:

$$k = \frac{1}{1+R\frac{dn}{dh}} = \frac{1}{1+R\frac{dN}{dh}10^{-6}} \quad (3.13)$$

where k is the effective earth's radius factor, R is radius of the earth in kilometres, $\frac{dN}{dh}$ is refractivity gradient and N is radio refractivity (Fashade *et al.,* 2019).

3.2.4 Field strength variability (FSV)

Radio refractivity correlates highly with radio field strength specifically at VHF bands. Between 30 and 300 MHz, a factor of 0.2 dB variation in field strength is usually adopted for every change in N_s. Maximum N_s(max) and minimum N_s(min) values were determined using N_s values obtained in each month of the year for all stations examined, from which the monthly range was calculated as:

$$\text{Monthly range} = N_{s(max)} - N_{s(min)} \quad (3.14)$$

Thus, calculation of field strength variability (FSV) in a station is determined from monthly ranges of N_s multiplied by 0.2 dB, using the relation (Oyedum, 2009):

$$\text{FSV} = N_{s(max)} - N_{s(min)} \times 0.2 \text{ dB} \quad (3.15)$$

3.3 Analysis of Data Collected

In situ observations of meteorological variables were obtained at 3 km height using automatic weather station for Bauchi and Yola. Data collected from January 2012 to December 2016 were averaged over each hour to give twenty-four data points representing diurnal variations for each

day. The hourly data for each day were further averaged to give a data point for the day and an average was taken over the month to give a data point for each month which was used to determine the monthly variations for each year. The corresponding months for each of the five years under study were then averaged to give the average seasonal variations for the period under study. Daily radio refractivity values for wet and dry months periods of the year were computed. The data analysis determined the refractivity, water vapour pressure, saturated water vapour pressure, modified refractivity, refractivity gradient, effective earth radius factor and field strength variability (FSV) using equations (3.3) – (3.15).

The atmospheric data for Kano were obtained at different height levels between 1.5 km and 21 km above the earth's surface but some atmospheric parameters were missing at various heights above 8 km. Therefore, the refractivity values computed in this thesis were only done at four (4) different height levels. These heights are 1.5 km, 3 km, 6 km and 8 km. The collected daily data at four different height levels for Kano were analysed to determine the refractivity, water vapour pressure, saturated water vapour pressure, modified refractivity, refractivity gradients, effective earth's radius factor and field strength variability (FSV) using equations (3.3) – (3.15). Results obtained for each study are presented in chapter four.

CHAPTER FOUR

RESULTS AND DISCUSSION

4.1 Analysis and Interpretation of Results

The data obtained from climatic observations at 5 minutes intervals in Bauchi and Yola were analysed with relevant mathematical tools to compute the values of radio refractivity for dry and wet terms of radio refractivity. The data obtained covered both dry and wet seasons of the year in Bauchi and Yola. Monthly and hourly mean values of surface radio refractivity were determined.

The monthly mean of radio refractivity over Kano, Bauchi and Yola for the months of January-December (2012-2016) were computed from radiosonde data and 5 minutes interval data of atmospheric pressure, relative humidity and temperature which were analysed and are hereby presented in this chapter. Seasonal variability of radio refractivity, modified refractivity, refractivity gradient, k-factor and field strength variability have been carried out. The results are presented and discussed in this chapter while the corresponding tables are given in Appendix A.

4.1.1 Monthly mean of hourly radio refractivity variations over Bauchi and Yola (2012-2016)

The hourly radio refractivity variation was explored for typical dry season and typical wet season months, as well as for both dry season and wet season in the study area. The typical dry season months observed are January and December while the wet season months are July and August. Figures 4.1- 4.4 show the daily mean hourly radio refractivity variations over Bauchi and Yola from 2012 to 2016. The hourly variation trends show the same variability pattern with high values of radio refractivity recorded at early morning hours and at nights and low values during day time or afternoon hours.

Figure 4.1 represents the radio refractivity for typical dry months in Bauchi. A sharp drop of radio refractivity was observed at 6:00 am with peak values of 275 N-units in January and 279 N-units in December were observed at 7:00 am in the morning and the minimum values of 258 N-units in January and 262 N-units in December were observed in the afternoon between 2:00 pm and 5:00 pm.

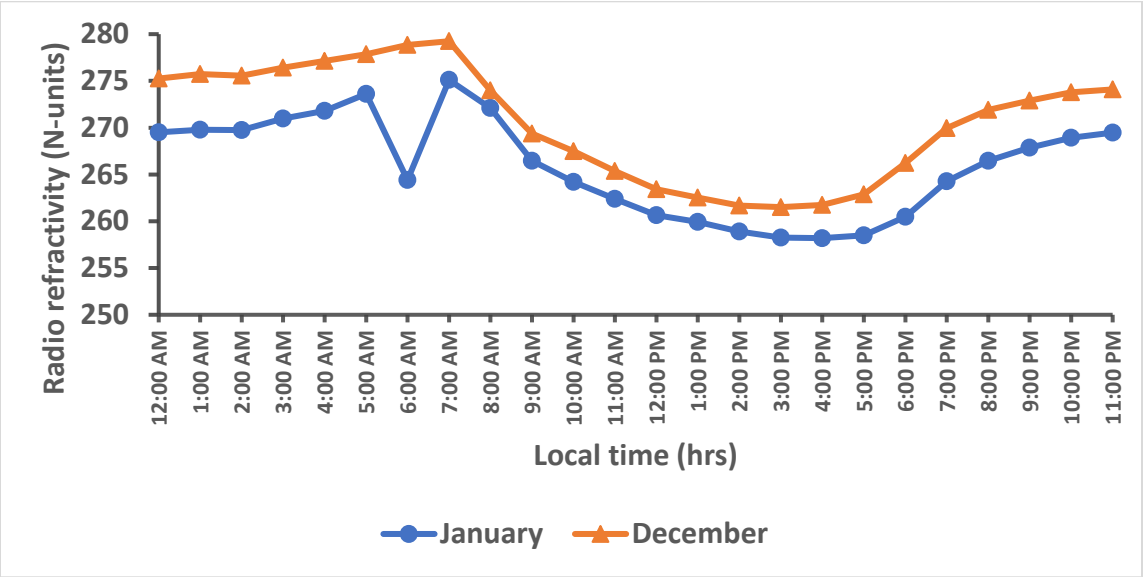

Figure 4.1: Hourly radio refractivity for typical dry season months in Bauchi

Figure 4.3 shows the radio refractivity for typical dry months in Yola. Peak values of 286 N-units in January and 288 N-units in December were observed between 6:00 am and 7:00 am in the morning and the minimum values of 270 N-units in January and 272 N-units in December were observed in the afternoon between 2:00 pm and 4:00 pm.

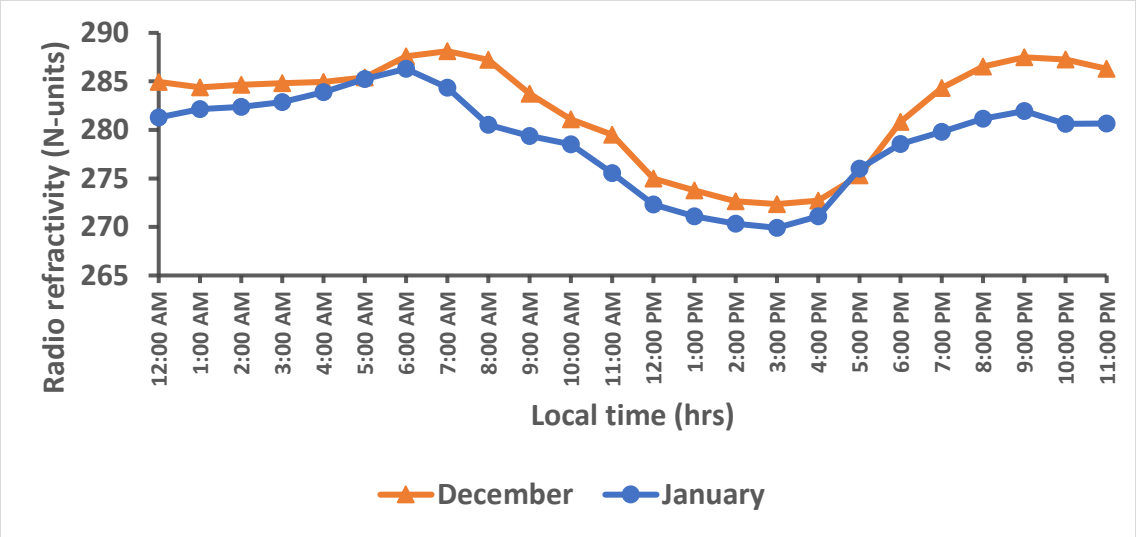

Figure 4.2: Hourly radio refractivity for typical dry season months in Yola

The radio refractivity for typical wet months in Bauchi is depicted in Figure 4.2. Peak values of 334 N-units in July between 6:00 am and 7:00 am and 339 N-units in August at 12:00 am, 3:00 am, 4:00 am, 9:00 pm to 11:00 pm were observed at early morning hours and at night, while minimum values of 303 N-units in July between 3:00 pm and 4:00 pm and 325 N-units in August at 4:00 pm were observed.

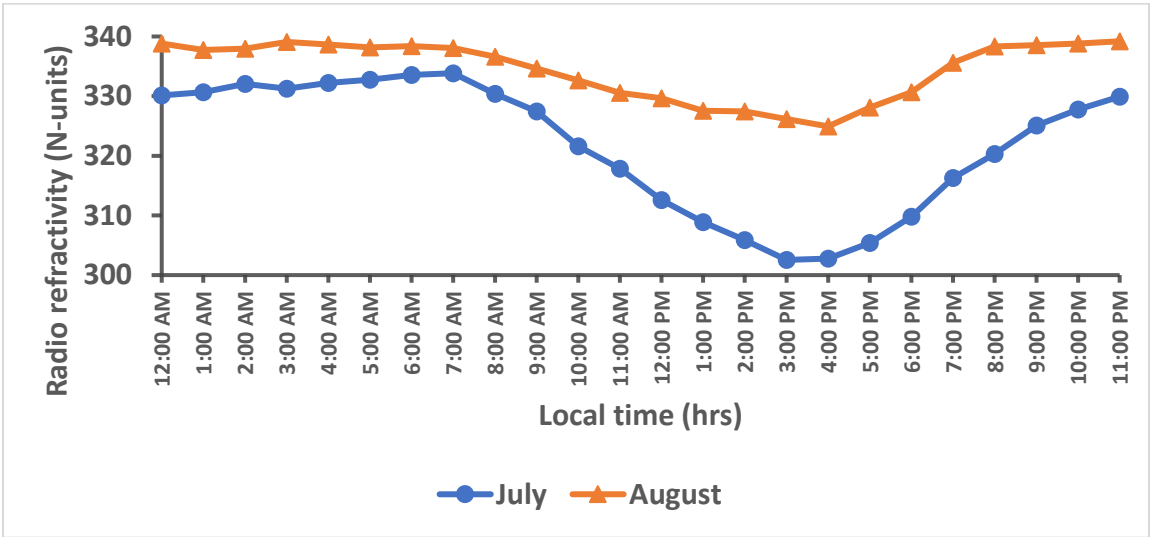

Figure 4.3: Hourly radio refractivity for typical wet season months in Bauchi

Figure 4.4 shows that in Yola the peak values of 352 N-units in July at 6:00 am and 356 N-units in August at 5:00 am, while the minimum values of 321 N-units in July at 2:00 pm and 327 N-units in August at 4:00 pm were observed during the wet season months. The peak values of radio refractivity observed at early morning hours and at late nights is as a result of high relative humidity and low temperature while the low values of radio refractivity observed during the day is due to low humidity and high temperature. The heating of the earth's surface by insolation increases towards noon; therefore, water vapour molecules in the atmosphere near the surface. As the water molecules get heated, they expand and move upwards leading to a decrease in relative humidity near the surface. Generally, as air temperature increases, relative humidity decreases while as air temperature drops, relative humidity increases.

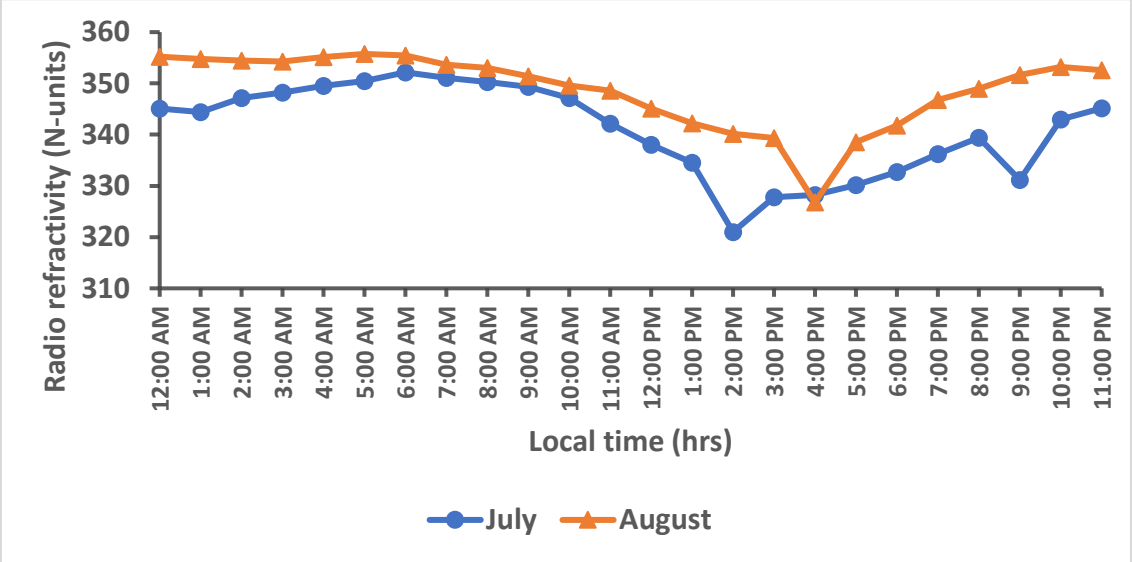

Figure 4.4: Hourly radio refractivity for typical wet season months in Yola

The study area under review experiences two seasons per annum: dry season and wet season. The mean hourly radio refractivity for dry and wet seasons is depicted in Figures 4.5-4.6. Figure 4.5 shows hourly radio refractivity variations for dry and wet seasons in Bauchi. A steady increase of

radio refractivity values from 12:00-5:00 am can be seen in the graph. Refractivity recorded a peak value of 276 N-units at 5:00 am with a sudden decrease at 6:00 am followed by a slight increase at 7:00 am, then a gradual decrease to 260 N-units at 3:00 pm local time, before a steady increase towards midnight for the dry term season. The wet term visibly shows a steady increase from mid-night towards the early morning hours and a rise to about 336 N-units at 6:00-7:00 am followed by a steady decrease to a minimum value of 314 N-units between 3:00-4:00 pm and a peak towards mid-night.

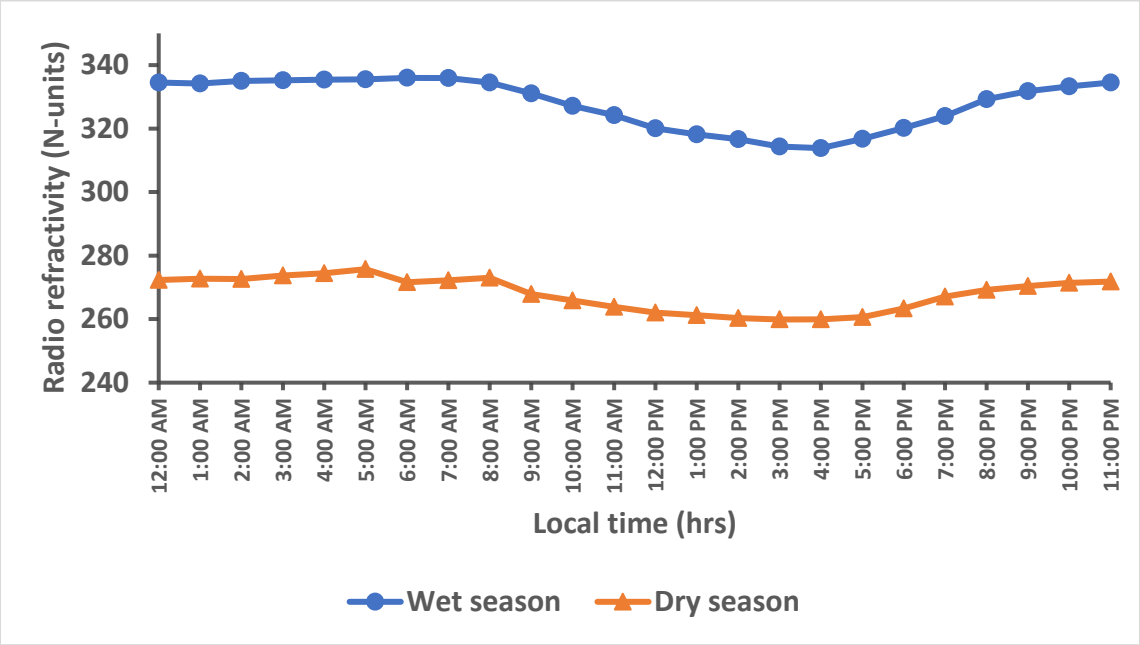

Figure 4.5: Mean hourly radio refractivity for dry and wet season months in Bauchi

Figure 4.6 depicts the radio refractivity variation of dry and wet season months in Yola. The dry season profile indicates a constant radio refractivity value of 283 N-units from 12:00-1:00 am and 284 N-units from 2:00-4:00 am, with a slight increase to 287 N-units at 6:00 am, a gradual drop from 7:00 am-12:00 pm was noticed. A fall which remained constant at 272 N-units from 1:00-2:00 pm decreased to a low refractivity value of 271 N-units at 3:00 pm local time and a steady increase towards midnight. A similar trend in variation was obtained for wet season months with

a maximum refractivity value of 354 N-units at 6:00 am, a steady decrease from 7:00 am-1:00 pm, reduced to a small decrease to about 331 N-units at 2:00 pm, followed by a rise at 3:00 pm and a decrease to a minimum value of 328 N-units at 4:00 pm and then increased gradually to a peak of 349 N-units towards mid-night. The high radio refractivity values observed in the early morning hours and at night is characterised by high relative humidity in the atmosphere while the lower refractivity values observed in the afternoon is as a result of high air temperature in the atmosphere.

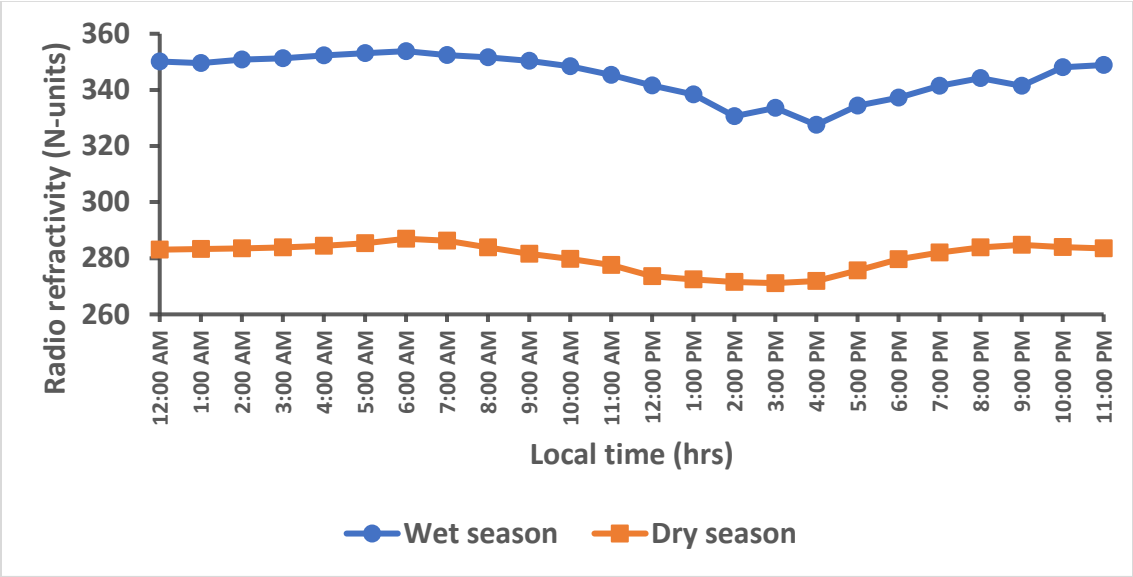

Figure 4.6: Mean hourly radio refractivity for dry and wet season months in Yola

4.2 Monthly Variation of Radio Refractivity over Bauchi, Yola and Kano (2012-2016)

Figure 4.7-Figure 4.9 depict the mean seasonal radio refractivity variations for five years (2012-2016) in Bauchi, Yola and Kano.

4.2.1 Radio refractivity in Bauchi

The seasonal variation of radio refractivity over Bauchi for a period of five years (2012-2016) is depicted in Figure 4.7.

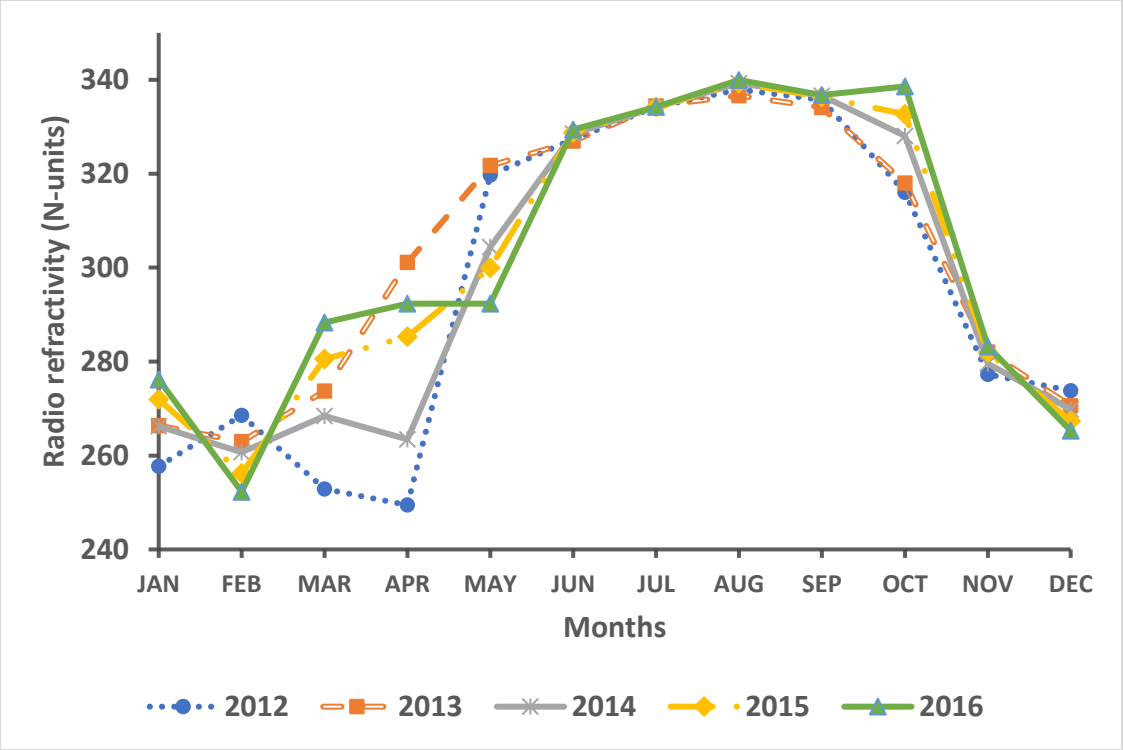

Figure 4.7: Monthly variation of radio refractivity in Bauchi

High radio refractivity values were observed during the rainy season months and low refractivity values during the dry season months. Thus, refractivity value was as low as 252 N-units in February and as high as 340 N-units in August.

4.2.2 Radio refractivity in Yola

Figure 4.8 illustrates the monthly variation of radio refractivity over Yola for a five-year period (2012-2016).

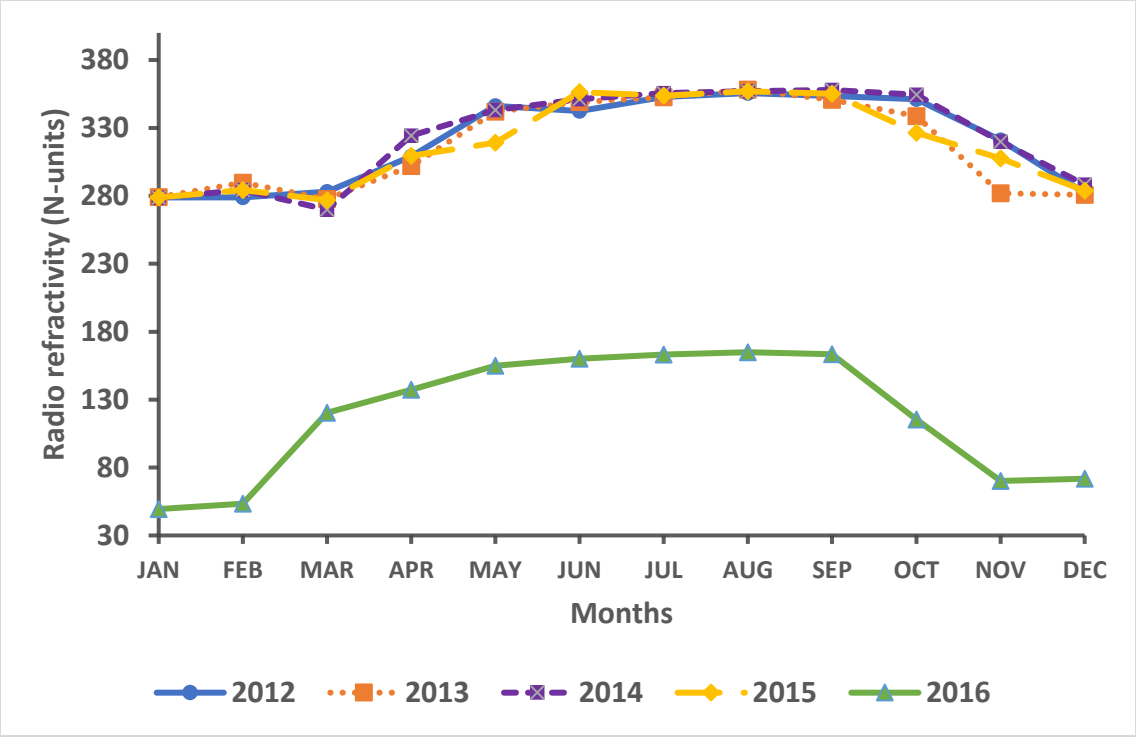

Figure 4.8: Monthly variation of radio refractivity in Yola over a period of 2012-2016

The figure above indicates a gradual increase in radio refractivity values from the month of January to July with a minimum refractivity value of 279 N-units in January for the years 2012, 2013, 2014 and 2015, while maximum refractivity values of 356 N-units, 358N-units, 357N-units and 165N-units were observed in August for the years 2012, 2013, 2015 and 2016 respectively with a steady drop in refractivity values from September to December. In 2014, a high refractivity value of 358 N-units was observed in September. In 2016, a low refractivity value of 49 N-units was observed in January. In 2016, Low atmospheric pressure was experienced. Depression (low atmospheric pressure) occurs when air rises and blows in an anticlockwise direction. When atmospheric pressure decreases, air rises and cools, then it condenses into water vapour to form clouds and precipitation.

4.2.3 Radio refractivity in Kano

Figure 4.9 depicts that five years (2012-2016) monthly variations of radio refractivity over Kano at four different height levels have been analysed and presented as follows.

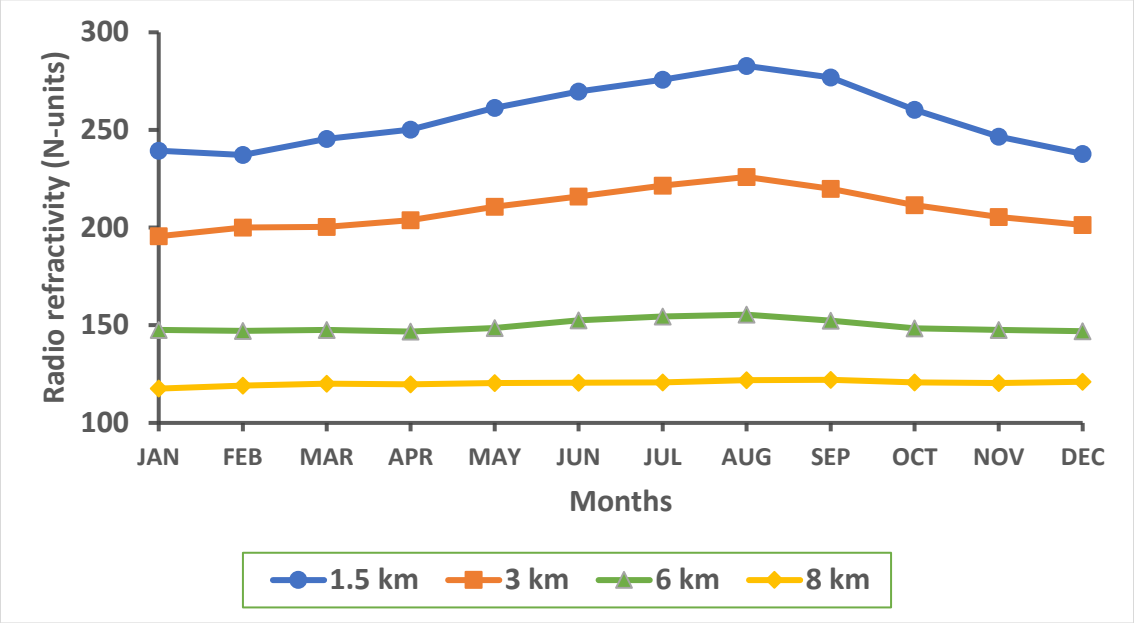

Figure 4.9: Monthly variation of radio refractivity in Kano at different heights

From Figure 4.9, a drop in refractivity value of 237 N-units was observed in February followed by a steady rise from March to a peak refractivity value of 283 N-units in August, then a gradual fall in September to December was observed at 1.5 km. At 3 km, refractivity values ranging from 196 N-units in January to 226 N-units in August were observed. Maximum refractivity value of 155N-units in December and February and minimum value of 147 N-units were observed at 6 km. A constant radio refractivity value of 122 N-units in August and September and low refractivity value of 118 N-units in January were observed at 8 km.

In the dry season, the Sahara Desert brings about dry and dust-laden Northeasterly winds which is responsible for the low radio refractivity values observed during the dry season, while the high

radio refractivity values observed during the rainy season are due to the influence of moisture laden Southwesterly winds from the Atlantic Ocean.

4.3 Mean Monthly Radio Refractivity Variations over Bauchi, Yola and Kano (2012-2016)

Figure 4.10 shows the monthly radio refractivity variations for all the three locations.

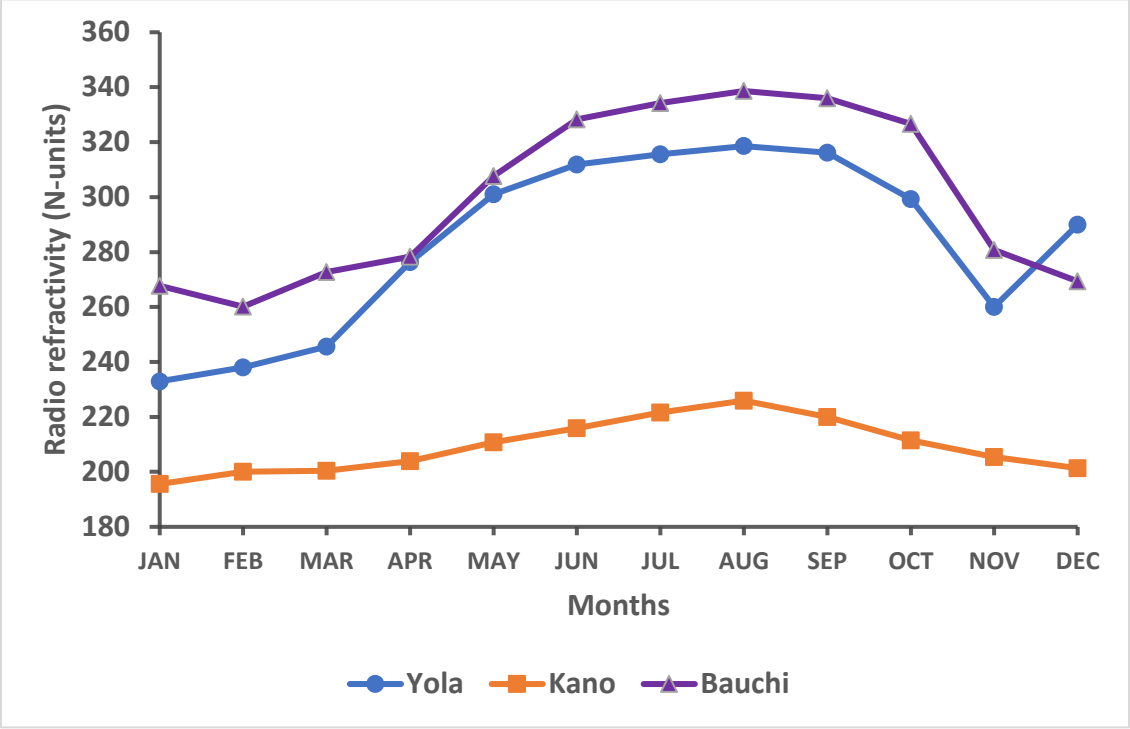

Figure 4.10: Mean monthly radio refractivity in Yola, Bauchi and Kano

Figure 4.10 shows that radio refractivity values are generally higher during the wet season months (May-October). This may be due to a constant increase in rainfall, which rises the moisture content in the atmosphere resulting to an increase of air humidity observed during that time of the year. Therefore, in the rainy season the locations might be under the influence of Southwesterly moisture laden maritime air due to South to North movement of the inter-tropical discontinuity (ITD) with the sun. The dry season months (November to April) reveals a drop in radio refractivity values due to dry and dust-laden Northeasterly winds which becomes dominant in the month of December

when harmattan sets in, resulting in lower refractivity values for the second and third peak dry months (January and December). Peak refractivity values were observed in August in Bauchi, Yola and Kano, while lowest refractivity values were observed in January (Kano and Yola) and February (Bauchi).

4.4 Modified Refractivity Variations across the Study Area

Modified refractivity and radio refractivity are similar. Hence, both vary in similar pattern during the dry and wet seasons. Figures 4.11-4.13 represent the monthly modified radio refractivity variations for Bauchi, Kano and Yola.

4.4.1 Modified radio refractivity in Bauchi

The mean monthly modified refractivity over Bauchi from 2012 to 2016 is shown in Figure 4.11.

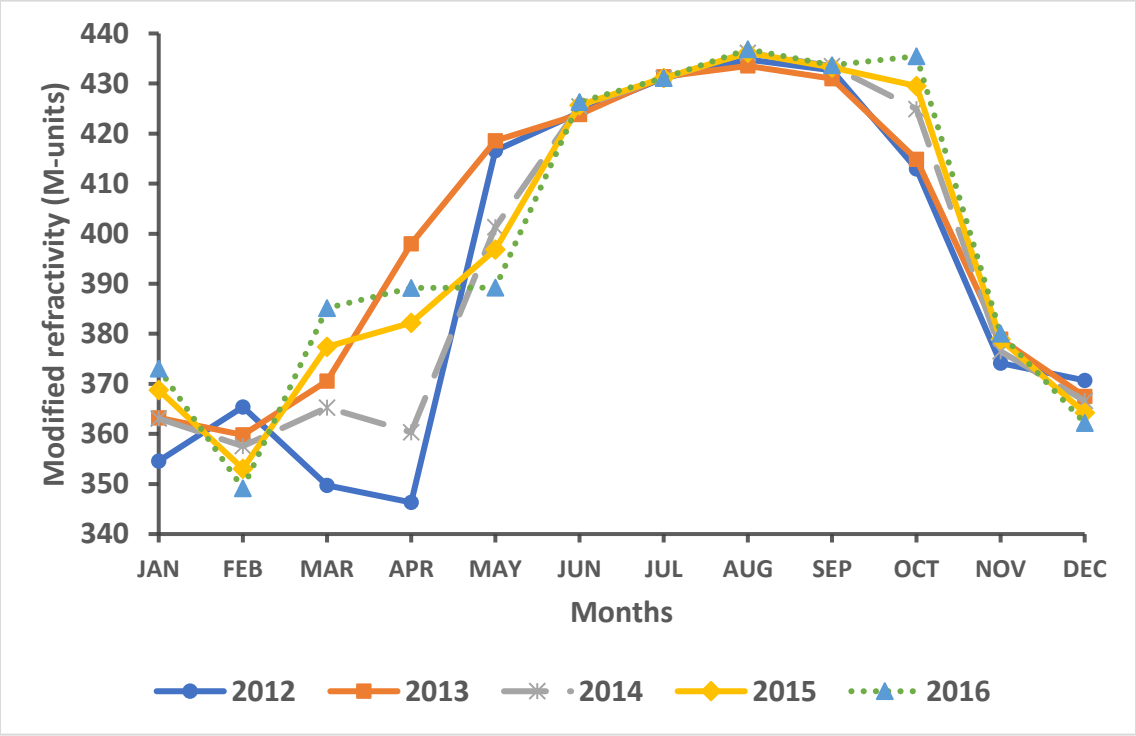

Figure 4.11: Mean seasonal variation of modified radio refractivity in Bauchi

Similar seasonal variations of modified refractivity were observed with the rainy season months (May-October) having peak modified radio refractivity values ranging between 389 M-units and 437 M-units, while the dry season months (November to April) have modified refractivity values ranging between 346 M-units and 380 M-units.

4.4.2 Modified radio refractivity over Yola

Monthly variations from 2012 to 2016 on modified radio refractivity in Yola is presented in Figure 4.12.

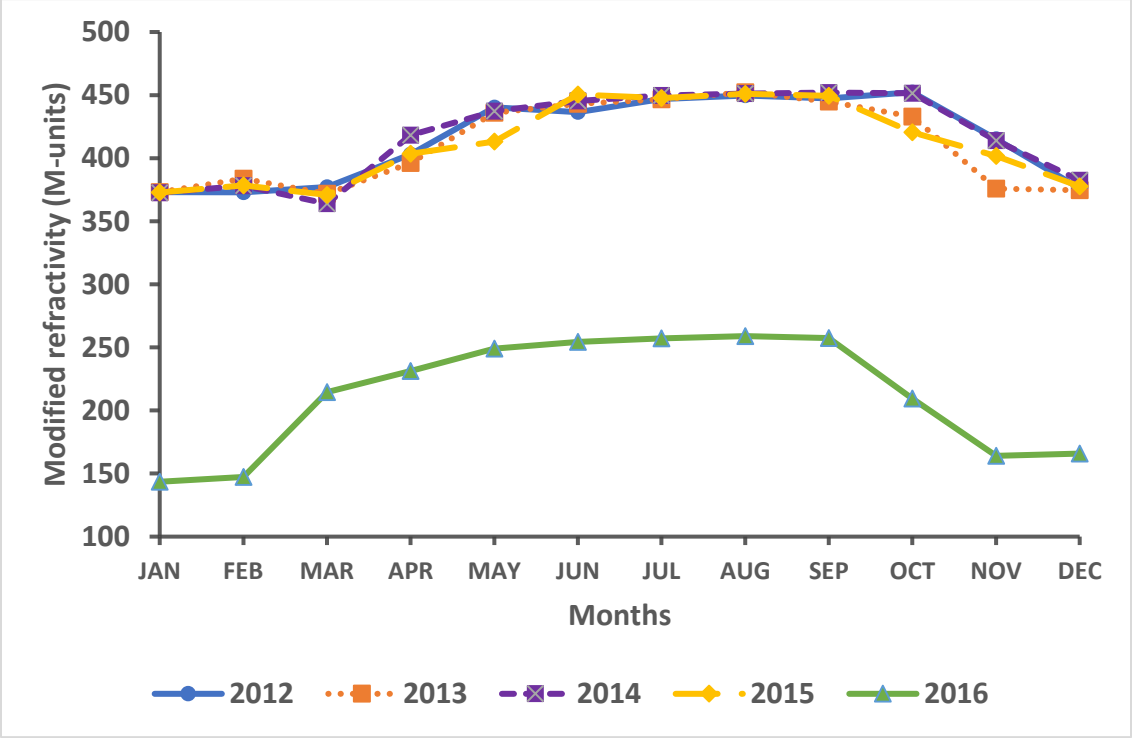

Figure 4.12: Mean seasonal variation of modified radio refractivity in Yola

Similar trends of modified radio refractivity was observed for the dry season months with refractivity values ranging from 143 M-units to 415 M-units and a sharp drop in radio refractivity value of 143 M-units was observed in January, 2016. Refractivity values ranging from 209 M-units to 452 M-units were observed for the wet season months.

4.4.3 Modified radio refractivity in Kano

Figure 4.13 presents the mean monthly modified radio refractivity variations in Kano for five years (2012-2016).

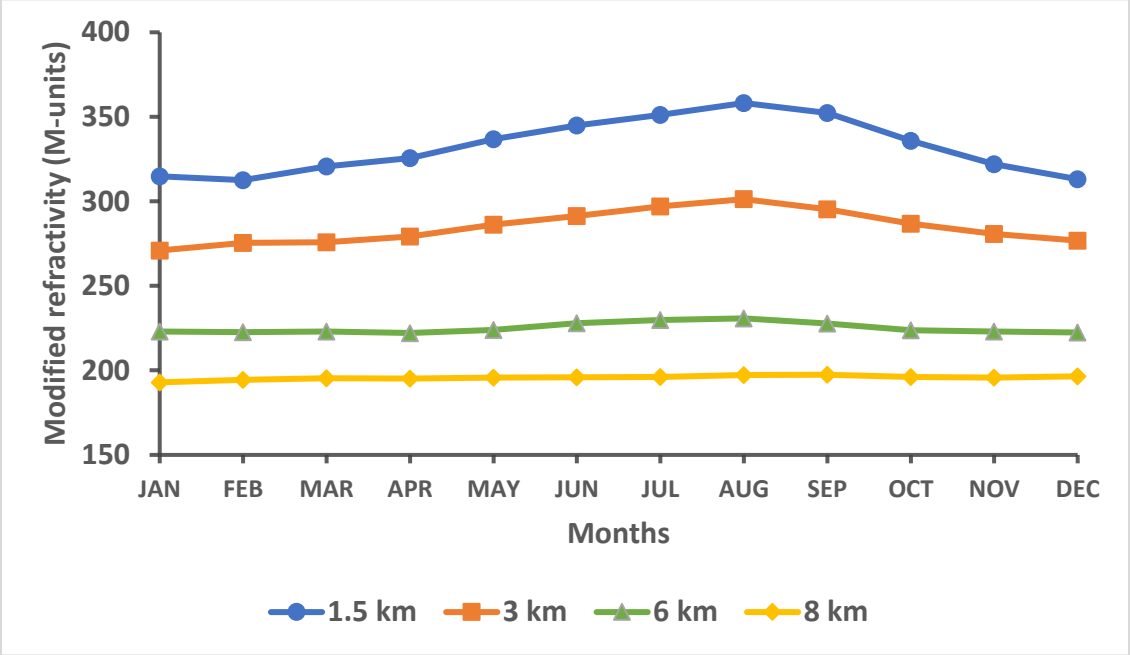

Figure 4.13: Mean seasonal variation of modified radio refractivity in Kano at different heights

Peak values ranging from 329 M-units to 358 M-units at 1.5 km, 286 M-units to 301 M-units at 3 km, 224 M-units to 231 M-units at 6 km and 196 M-units to 197 M-units at 8 km were observed during the wet season months, while refractivity values ranging from 313 M-units to 326 M-units at 1.5 km, 271 M-units to 281 M-units at 3 km, 222 M-units to 223 M-units at 6 km and 193 M-units to 196 M-units at 8 km were observed during dry season months.

4.5 Radio Refractivity Gradient (RRG)

The mean monthly variation of radio refractivity gradient in Bauchi, Yola and Kano are shown in Figures 4.14-4.16.

4.5.1 Radio refractivity gradient in Bauchi

Figure 4.14 presents the mean monthly variation of radio refractivity gradient in Bauchi from 2012 to 2016.

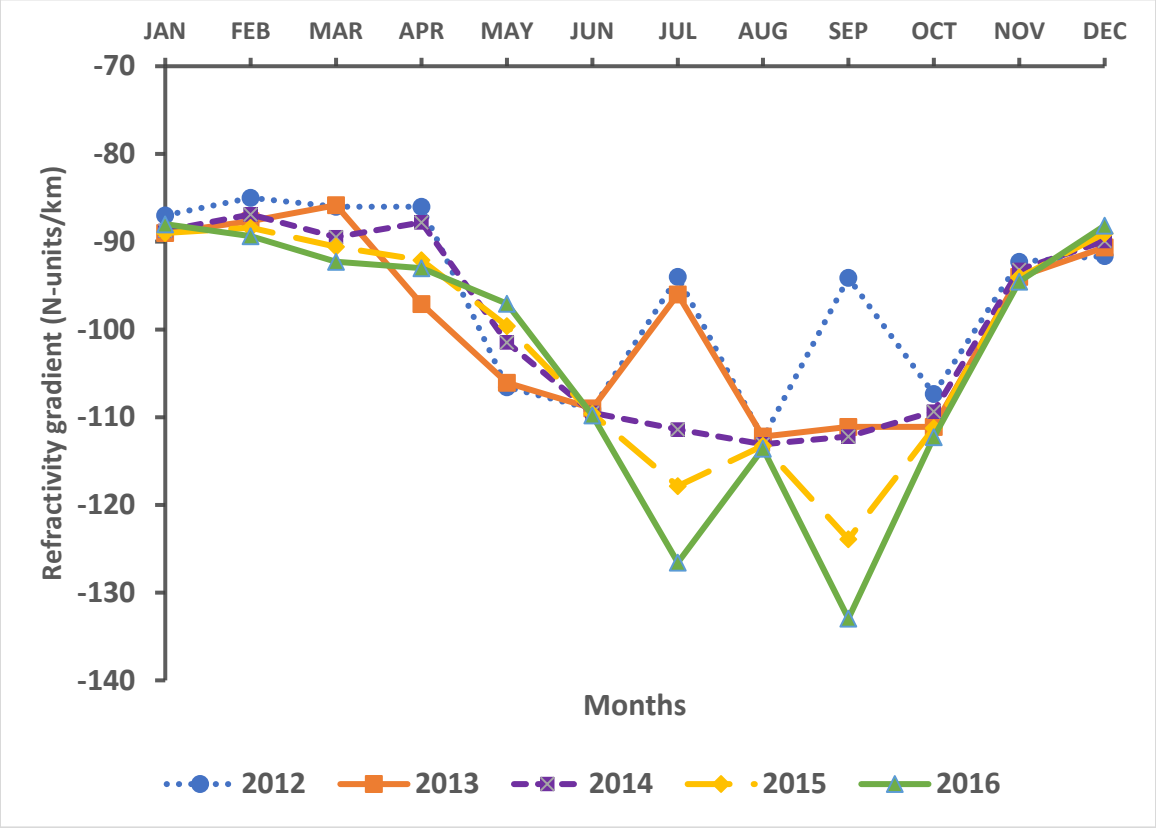

Figure 4.14: Mean monthly variation of radio refractivity gradient in Bauchi

Figure 4.14 clearly shows the refractivity gradient values for the dry season months ranging between -97 N-units/km to -85 N-units/km. The wet season months have refractivity gradient values ranging between -124 N-units/km to -94 N-units/km. The result indicates that super-refractive condition was prevalent in Bauchi during the period of the study.

4.5.2 Radio refractivity gradient in Yola

Figure 4.15 depicts the mean monthly radio refractivity gradient in Yola from (2012-2016).

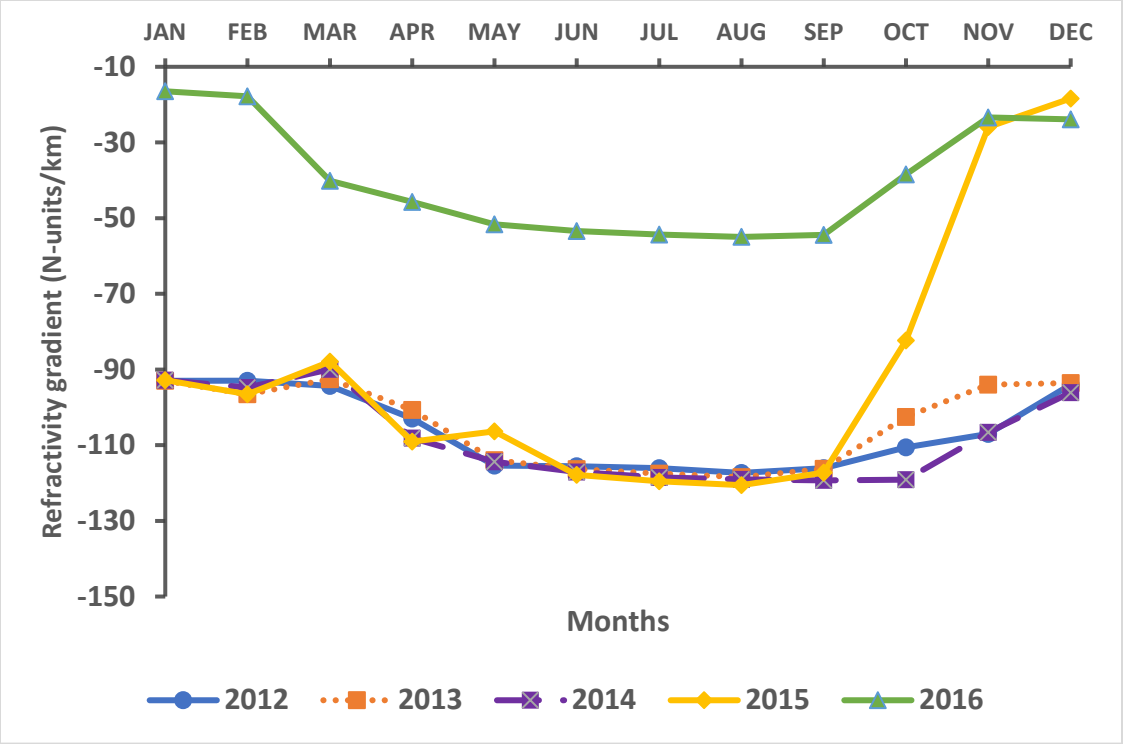

Figure 4.15: Mean monthly variation of radio refractivity gradient over Yola

Figure 4.15 represents refractivity gradient values varying from -109 N-units/km to -16 N-units/km for the dry months, while the wet months have refractivity gradient values varying from -121 N-units/km to -55 N-units/km. Therefore, the atmospheric condition in Yola was super refractive during the study period.

4.5.3 Radio refractivity gradient in Kano

Figure 4.16 presents the mean monthly variation of radio refractivity gradient in Kano for the five-year study period (2012-2016) at 3 km, 6 km and 8 km.

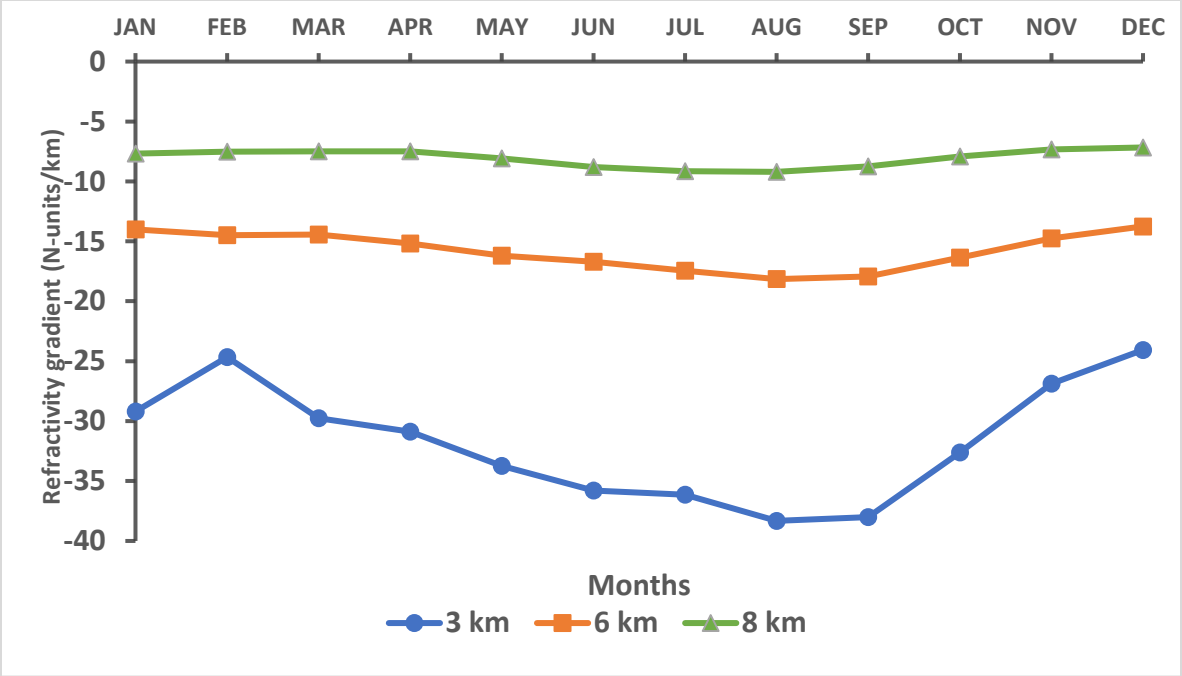

Figure 4.16: Mean monthly variations of radio refractivity gradient over Kano at different heights

Figure 4.16 shows that refractivity gradient varies from -24 N-units/km in December to -38 N-units/km in August and September at 3 km. At 6 km, -14 N-units/km in December, January, February and March to -18 N-units/km in August and September; and it varied from -7 N-units/km in November and December to -9 N-units/km in June, July, August and September at 8 km. From the results, it was observed that Kano could experience sub-refraction from 3 km upwards in the atmosphere.

4.6 The Effective Earth Radius Factor (k-factor)

Refractivity gradient of the first kilometres directly above the earth's surface was applied to determine the effective earth radius factor which is dependent on the type of season as stated in (Fashade *et al.*, 2019). Mean seasonal k- factor and radio refractivity are shown in Figures 4.17-4.19.

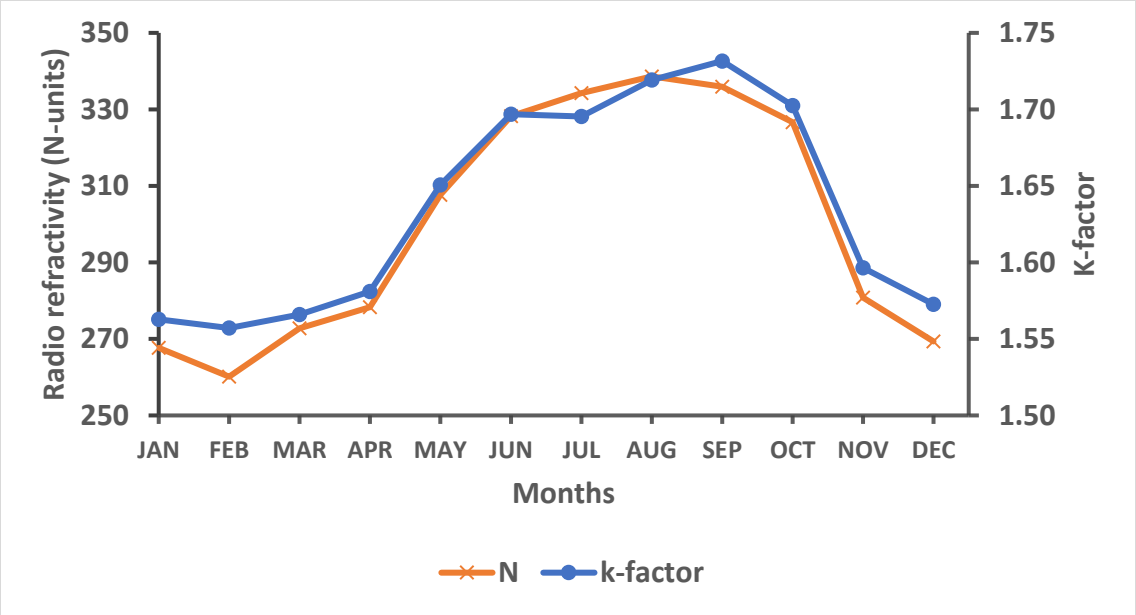

Figure 4.17: Variation of mean monthly radio refractivity and k-factor over Bauchi

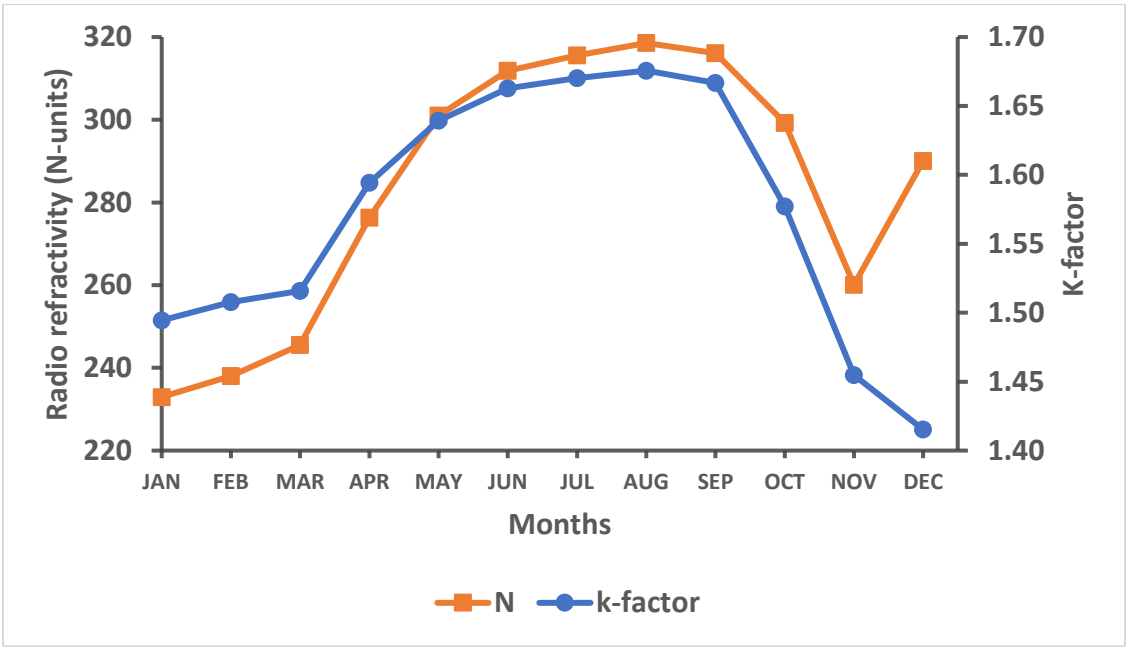

Figure 4.18: Variation of mean monthly radio refractivity and k-factor over Yola

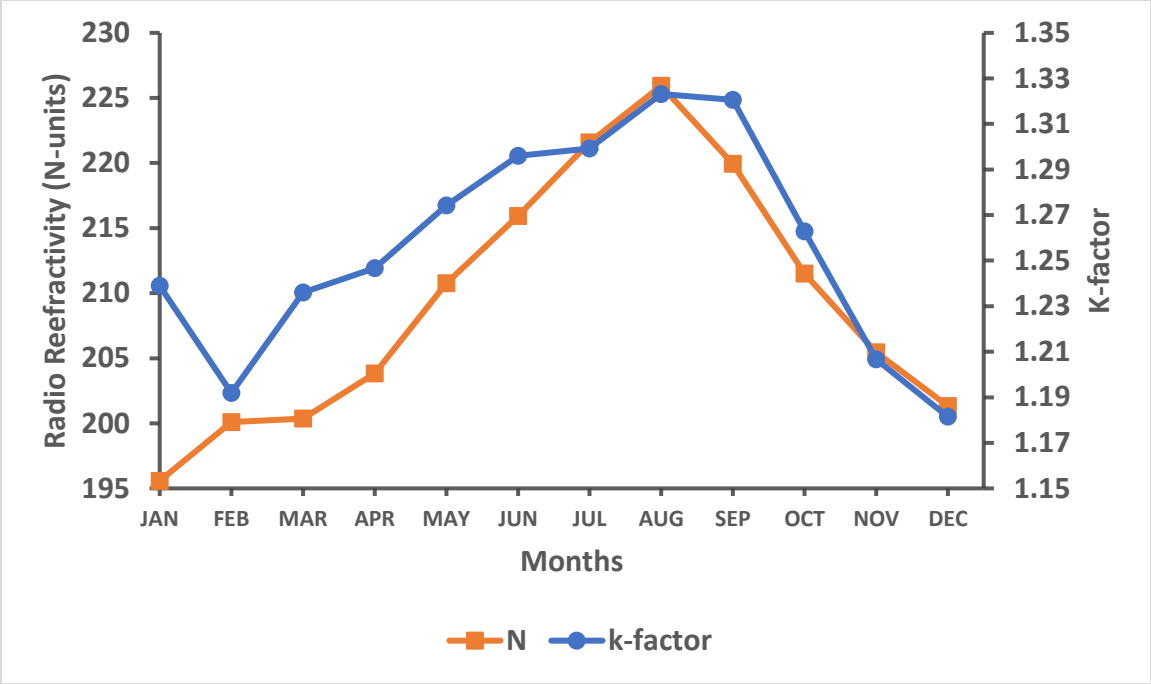

Figure 4.19: Variation of mean monthly radio refractivity and k-factor over Kano

Figures 4.17 and Figure 4.18 clearly show that k-factor values decrease with a decrease in radio refractivity. Both locations (Bauchi and Yola) indicate high k- factor values throughout the dry season months and low k-factor values throughout the rainy season months.

In Figure 4.19, k-factor shows a similar trend with radio refractivity in Kano. Peak k-factor value occurs during the rainy season period of the year, while a drop in k-factor value occurs during the dry season period of the year. From the result, it shows that k-factor increases with an increase in radio refractivity in Kano.

4.6.1 Mean k-factor values over Bauchi, Kano and Yola

Figure 4.20 is the mean k-factor for all the stations under review from 2012 to 2016.

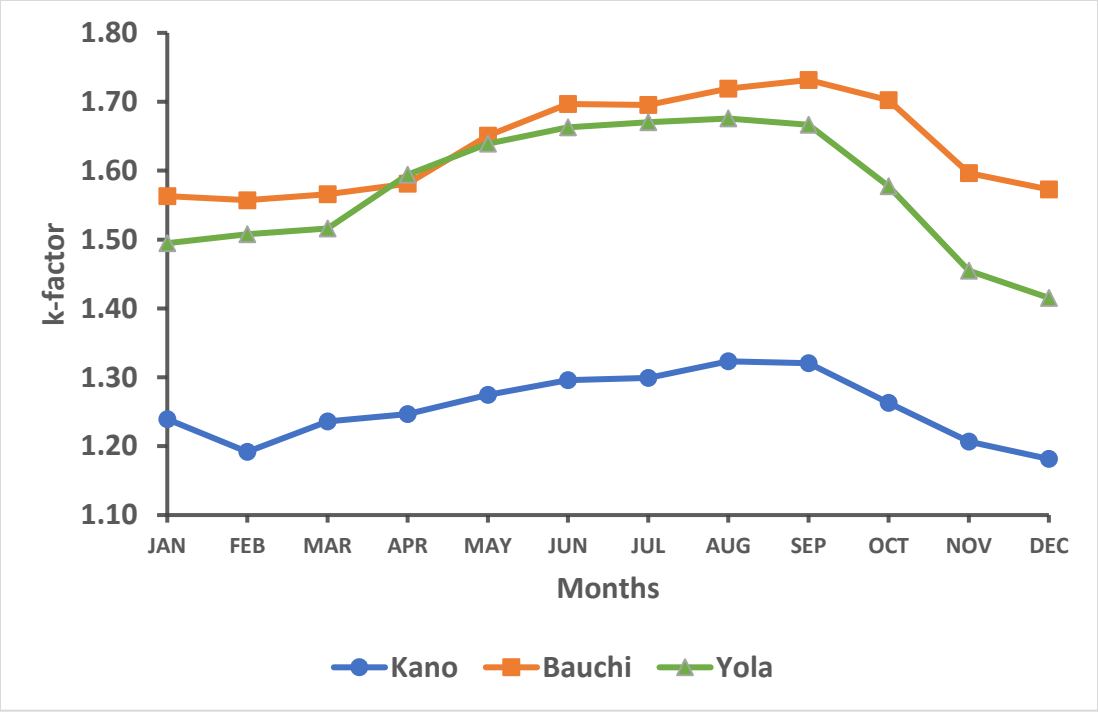

Figure 4.20: Mean monthly k-factor variations in Bauchi, Kano and Yola

Figure 4.20 shows that the average k-factor values for the dry and wet seasons ranged from 1.567 to 1.70, 1.50 to 1.65 and 1.18 to 1.32 in Bauchi, Yola and Kano respectively. The k-factor values were taken with reference to 3 km for the stations under review. Bauchi and Yola have similar k-factor values which depict that they are under the same climatic conditions while a different climatic condition was depicted in Kano.

4.7 Radio Field Strength Variability (FSV)

The mean monthly radio field strength variability and radio refractivity are shown in Figures 4.21-4.23.

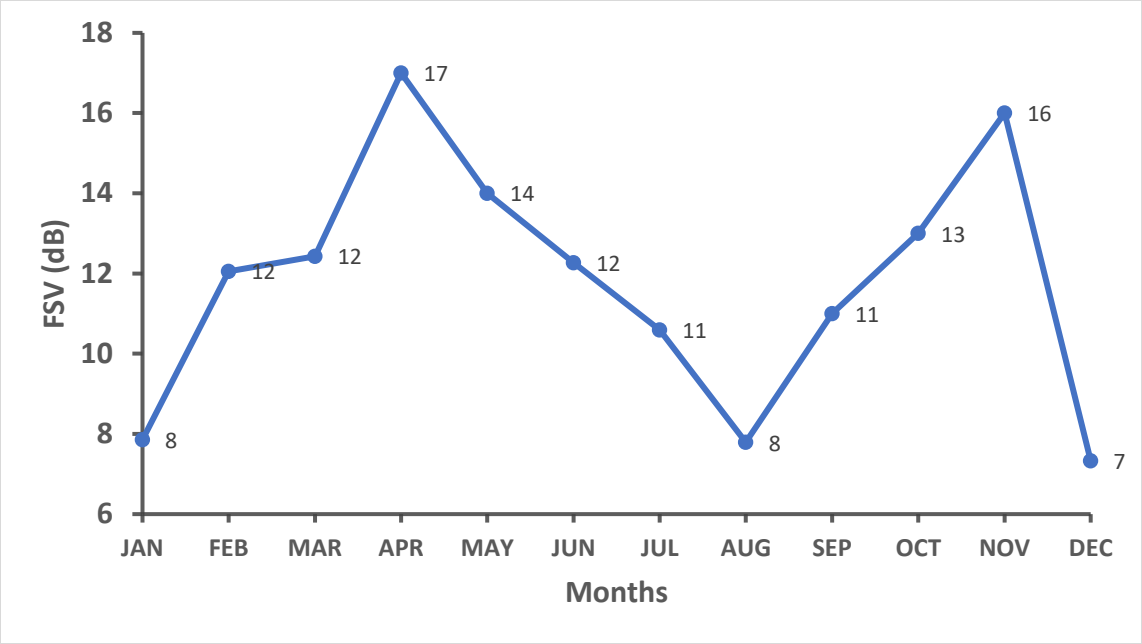

Figure 4.21: Mean monthly field strength variability over Bauchi

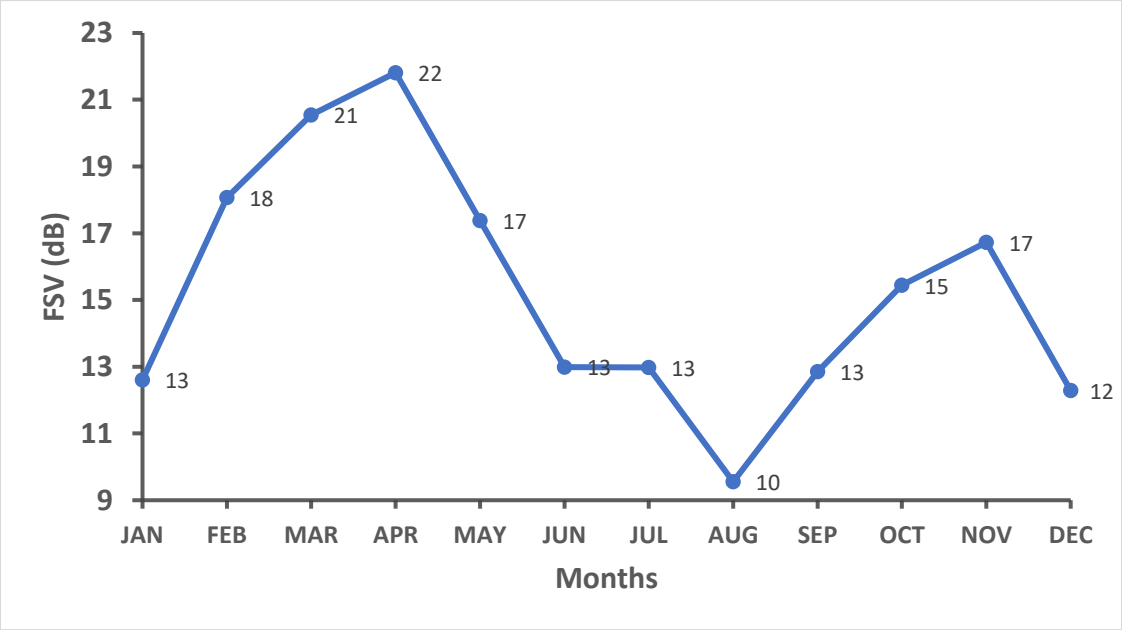

Figure 4.22: Mean monthly field strength variability over Yola

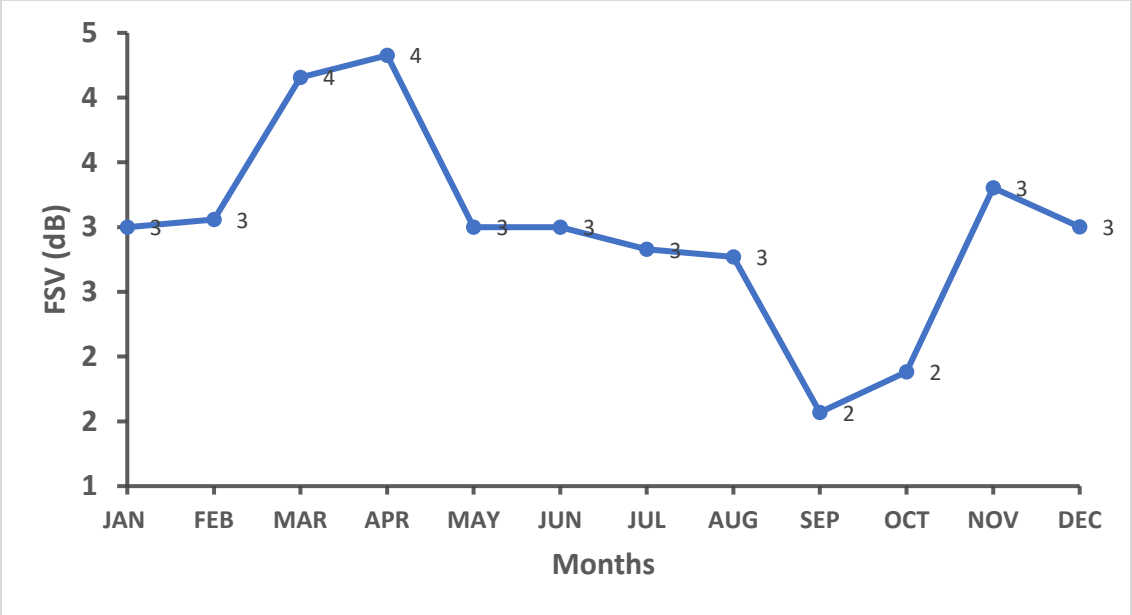

Figure 4.23: Mean monthly field strength variability over Kano

Figure 4.21-Figure 4.23 show FSV values ranging from 7 dB to 17 dB, 10 dB to 22 dB and 2 dB to 4 dB in Bauchi, Yola and Kano respectively. Field strength variability is characterised by high decibels in dry season months and low decibels in wet season months which may be ascribed to the existence of high temperature during the dry season of the year and high air humidity during the wet season of the year.

4.8 Summary of Findings

These are the summary of findings in this work:

1. The hourly refractivity values obtained for dry and wet season months showed a decrease in the afternoon and an increase during the early morning hours and at night.
2. The monthly radio refractivity trends showed an increase in radio refractivity values during the wet season months and a decrease during the dry season months.

3. The values of modified refractivity computed reveal that the wet season months have higher modified refractivity than the dry months.
4. Refractivity gradient values show that sub-refraction occurred in Kano while super refraction occurred in Bauchi and Yola.
5. The values of computed k-factor showed that abnormal conditions of sub-refraction and super-refraction were experienced in the locations under review.
6. The computed Field Strength Variability showed that dry season months have higher values than the wet season months.

CHAPTER FIVE

CONCLUSION AND RECOMMENDATIONS

5.1 CONCLUSION

Five-year data collected from NASRDA and NIMet were used to determine radio refractivity which encompasses diurnal and seasonal variations. Mean hourly radio refractivity values of 268 N-units in dry season and 328 N-units in wet season were observed in Bauchi, while refractivity values of 281 N-units in dry season and 345 N-units in wet season were observed in Yola. The values obtained for both dry and rainy season months indicated an increase in radio refractivity values during early morning hours and at night with a decrease in refractivity values in the afternoon. Mean monthly radio refractivity values ranged from 272 N-units to 329 N-units in Bauchi and 249 N-units to 310 N-units in Yola. In Kano, refractivity values ranged from 243 N-units to 271 N-units at 1.5 km height, 201 N-units to 218 N-units at 3 km height, 147 N-units to 152 N-units at 6 km height and 120 N-units to 121 N-units at 8 km height. The mean monthly radio refractivity variation for the rainy season months depicts a higher radio refractivity values than the dry season months. Radio refractivity determines how far radio signal will travel within the atmosphere.

The computed modified refractivity also shows seasonal variability pattern. However, the values of modified refractivity computed were higher than those of radio refractivity. The atmosphere over Bauchi and Yola was observed to be super-refractive, while the atmosphere in Kano was sub-refractive from the computed result. Refractivity gradient values in Bauchi ranged between -115 N-units/km in September and -87 N-units/km in February, while refractivity gradient values ranged from -106 N-units/km in August to -65 N-units/km in December in Yola. In Kano,

refractivity gradient at surface level ranged from -24 N-units/km in December to -38 N-units/km in August at 3 km. At 6 km height, values ranged from -14 N-units/km in December to -18 N-units/km in August. At 8 km height, values ranged from -7 N-units/km in November to -9 N-units/km in June.

Line-of-sight (LOS) propagation can be compromised by considerable variation in k- factor. A minute difference in k-factor value generates abnormal propagation which leads to sub-refraction, super-refraction and ducting. An average k-factor of 1.57 in Yola and 1.67 in Bauchi which agrees to the anomalous propagative condition of super-refraction was observed, while Kano recorded an average k-factor value of 1.26 which agrees to the propagative condition of sub-refraction. In the design and planning of radio links in radio propagation, k-factor is applied by radio engineers to obtain sufficient path clearance.

Generally, radio field strength variation display fluctuations during wet months and dry months. Wet season months exhibited low FSV due to high increase in water vapour content in the atmosphere, while dry season months recorded high FSV. Yola and Bauchi recorded low values of 10 dB and 8 dB respectively in August, while high values of 22 dB and 15 dB were recorded respectively in April. For Kano, a low value of 2 dB was recorded in September and October, while 5 dB was recorded in June. An average value of 15 dB in Yola, 12 dB in Bauchi and 3 dB in Kano were recorded during the period of study. FSV will improve Field performance and ensure increased reliability of planned radio links.

5.2 RECOMMENDATION

The knowledge obtained from this study will provide radio engineers with substantial information needed for the design of communication systems in the study area which will serve as a vital platform in determining the coverage and quality of VHF, UHF and microwave signals.

Therefore:

1. Since radiosonde data are hard to obtain and are also very expensive, government agencies should provide subsidies for research purposes. Further studies should be encouraged in the same field with extensive data of 10 to 15 years or more.
2. Incomplete data obtained from both CAR-NASRDA and NIMet needs to be addressed extensively for the determination of accurate result. Since radiosonde data are hard to obtain and are also very expensive, an appropriate and accurate system for logging of data should be adopted to avoid fragmentation of data received for research purposes.
3. Surface data is vital in radio refractivity computations. A limitation was experienced due to lack of availability of surface data for Kano which lead to the computation of refractivity gradient from 3 km and above. CAR-NASRDA and NIMet should provide more weather stations and make all atmospheric data available for research work.

5.3 CONTRIBUTION TO KNOWLEDGE

The study determined the refractivity profiles of Yola, Bauchi and Kano which will guide propagation links in the region; the refractivity gradients revealed the prevailing propagation conditions while the k-factor showed that radio links in Yola and Bauchi will generally have clearance from surface-based obstacles under the prevailing refractivity conditions, but more attention should be given to radio links in Kano where value of k-factor could sometimes be exceptionally low. The study also showed that field strength variability in the region is higher in dry season but very low in wet season, which will also guide network providers in the region.

REFERENCES

Adebanjo, T. I. (1977). A semi-empirical radio refractive index variation over Nigeria. *Nigerian Institute of Physics Bulletin*, 2(2), 69-78.

Adedayo, K. D. (2016). Statistical analysis of the effects of relative humidity and temperature on radio refractivity over Nigeria using satellite data. *African Journal of Environmental Science and Technology*, 10(7) 221-229.

Adediji, A.T., & Ajewole, M. (2008). Vertical profile of radio refractivity gradient in Akure South-West Nigeria. *Progress in Electromagnetics Research C*, 4, 157-68.

Adeyemi, B. (2004). Tropospheric radio refractivity over three Radiosonde Stations in Nigeria. *Ife Journal of Science*, 6(2), 167-176.

Adeyemi, B., & Emmanuel, I. (2011). Monitoring tropospheric radio refractivity over Nigeria using CM –SAF data derived from NOAA-15, 16 and 18 satellites. 92.60.hf.

Afullo, T. J., & Odedina, P. K. (2004). Effective earth radius factor characterization for line of sight paths in Botswana. In 2004 IEEE Africon. 7thAfricon Conference in Africa (IEEE Cat. No.04CH37590), (vol.1, pp. 227-231). IEEE.

A quick derivation relating altitude to air pressure. (2011). Achieved from https://www.psas.pdx.edu on 28th September 2011 at way back machine by Portland State Aerospace Society (PSAS).

Akpootu, D. O., Iliyasu, M. I., Mustapha, W., Aruna, S., & Yusuf, S. O. (2017). The influence of meteorological parameters on atmospheric visibility over Ikeja, Nigeria. *Archives of Current Research International*, 9(3), 1-12.

Ayantunji, B. G., Okeke, P. N., & Urama, J.O. (2011). Diurnal and seasonal variation of surface refractivity over Nigeria. *Progress in Electromagnetics Research B*, 30, 201-22.

Barclay, L. (2003). Propagation of radio waves (2nd edition). The Institution of Electrical Engineers, London, pp. 103-127.

Balogun, E. E. (1981). Seasonal and spatial variations in thunderstorm activity over Nigeria. *Monthly weather review*, 36(7), 192-197.

Balogun, E. E., & Adedokun, J. A. (1986). On the variations in precipitable water over some West African stations during the special observation period of WAMEX. *Monthly weather review*, 114(4), 772-776.

Bauchi State https://en.wikipedia.org/wiki/Bauchi-State retrieved on 19th May, 2020.

Bean, B. R., & Dutton, E. J. (1968). Radio Meteorology. Dover Publication Company, New York. pp. 259-273.

Bean, B. R., & Thayer, G. D. (1963). Comparison of observed atmospheric radio refraction effects with values predicted through the use of surface weather observations. Space Flight Testing Conference p. 69, 1963.

Bolton, D. (1980). The computation of equivalent potential temperature. *Monthly weather review*, 108(7), 1046-1053.

Buck, A. L. (1981). New equations for computing vapor pressure and enhancement factor. *Journal of Applied Meteorology and Climatology*, 20(12), 1527-1532.

Byjus. https://byjus.com/snells-law-formula/a retrieved on 22nd October, 2020.

Earth's atmosphere composition: Nitrogen, Oxygen, Argon and $C0_2$. www.Earthhow.com/earth-atmosphere-composition/ retrieved on 22nd October, 2019.

Fashade, O. O., Omotosho, T. V., Akinwumi, S. A., & Olorunyomi, K. P. (2019). Refractivity gradient of the first 1 km of the troposphere for some selected stations in six geo-political zones in Nigeria. In IOP Conference Series: *Materials Science and Engineering*, 640(1), 012087.

Flavell, R. G., & Lane, J. A. (1962). The application of potential refractive index in tropospheric wave propagation. *Journal of Atmospheric Terrestrial Physics*, 24(1), 47–56.

Hall, M. P. (1980). Effects of the troposphere on radio communications. Stevenage Herts England Peter Peregrines Ltd. Institute of Electrical and Electronics Electromagnetic Waves Series, 8.

Hampshire, D. P. (2018). A derivation of Maxwell's equations using the Heaviside notation. *Philosophical Transactions of the Royal Society A: Mathematical, Physical and Engineering Sciences*, 376(2134), 20170447.

Igwe, K.C., & Adimula, I. A. (2009). Variation of surface radio refractivity and radio refractive index gradients in the Sub- Sahel. *Nigerian Journal of Space Research*, 6, 135-144.

Igwe, K.C., Tukur, I. M., & Eichie, J. O. (2018). Radio refractive index and refractive index gradients variation in a tropical environment. 3rd International Engineering Conference, pp. 239-243.

Ionosphere https://en.m.wikipedia.org/wiki/ionosphere retrieved on 22nd November, 2019.

International Telecommunication Union recommendation, ITU-R (2015). The radio refractive index: Its formula and refractivity data. ITU Radio Communication Assembly, ITU-R P-Series, P.453-11.

International Telecommunication Union recommendation, ITU-R (2019). The radio refractive index: Its formula and refractivity data. ITU Radio Communication Assembly, ITU-R P-Series, P.453-14.

International Civil Aviation Organization. Manual of the ICAO Standard Atmosphere. (1993). Third Edition, Doc 7488-CD.

Jacob, D. J. (1999). Introduction to atmospheric chemistry. Princeton University Press.

Jidong, G., Keit, B., & Ming, X. (2008). Variation of radio refractivity with respect to moisture and temperature and influence on radar ray path. *Advance in Atmospheric Sciences*, 25(6), 1098-1106.

Kano State https://en.wikipedia.org/wiki/Kano-State retrieved on 19th May, 2020

Kolawole, L. B., & Owonubi, J. J. (1982). The surface radio refractivity over Africa. Nigeria *Journal of Science*, 16(1-2), 441-454.

Kolawole, L. B. (1980). Climatological variations of surface radio refractivity in Nigeria. *Nigerian Institute of Physics Bulletin*, 4, 97–117.

Korak-Shaha, P. N. (2003). The Physics of Earth and its Atmosphere. John and Sons Inc., New York, USA.

Lane, J. A., & Bean, B. R. (1963). A radio meteorological study. Part I: Existing radio meteorological parameters; Part II: An analysis of VHF field strength variations and refractive index profiles; Part III: a new turbulence parameter, *Journal of Research of the National Bureau of Standards D*, 67(6), 589-604.

Lawrence, M. G. (2005). The relationship between relative humidity and dewpoint temperature in moist air: A simple conversion and applications. *Bulletin of the American Meteorological Society*, 86(2), 225-233.

Layers of the atmosphere https://niwa.co.nz/education-and training/schools/students/layers retrieved on 20th, October, 2020.

Layers of the earth's atmosphere www.scied.ucar.edu/learning-zone/atmosphere/layers-earths-atmosphere retrieved on 3rd March, 2015.

Lide, D. R. (2005). CRC Handbook of chemistry and physics, internet version.

Mahdi, Qaysar & Salih, Idris. (2017). Evaluation of Mobile GSM Performance under Different Atmospheric Propagation Models. Eurasian Journal of Science and Engineering. V3i2. 151. 10.23918/eajse.v3i2p151.

Martin, G., & Vaclav, K. (2011). Atmospheric refraction and propagation in lower troposphere. *Electromagnetic waves*, 139-156.

Misme, P. (1960). Models of the atmospheric radio refractive index. *Proceedings of the Institute of Radio Engineers*, 48(8), 1499-1501.

Monebhurrun, V. (2021). IEEE Standard 1502-2020: IEEE Recommended Practice for Radar Cross-section Test Procedures (Stand on Standards). *IEEE Antennas and Propagation Magazine*, 63(2), 106-106.

Okpani, P. E., Nwofe P. A., & Chukwu N. O. (2015). Effect of secondary radio-climatic variables on signal propagation in Nsukka, Nigeria. *International Research Journal of Natural Sciences* 3 (2), 9-17.

Owolabi, I. E., & Williams, V. A. (1970). Surface radio refractivity patterns in Nigeria and the southern Cameroons. *Journal of West Africa Science Association*, 15(1), 3-17.

Oyedum, O. D., & Gambo, G. K. (1994). Surface radio refractivity in northern Nigeria. *Nigerian Journal of Physics*, 6, 36-41.

Oyedum, O. D. (2009). Seasonal variability of radio field strength and radio horizon in Northern and Southern Nigeria. *Nigerian Journal of Pure and Applied Physics*, 5(1), 97-104.

Oyedum, O. D., Igwe, K. C., Eichie, J. O., & Moses, A. S. (2010). Reduced to sea level refractivity in Minna, Central Nigeria. *Journal of Natural and Applied Sciences.*

Oyedum, O. D. (2005). Duct-induced microwave link degradation in Nigeria part II: minimization factors. *Book of Readings:* 20th-23rd November, 2005, 2,168.

Researchgate. Positions in Nigeria of Kano, Bauchi and Yola https://www.researchgate.net/figure/map-of-Nigerian-left-and-map-of-kano-Bauchi-and-Yola retrieved on October, 2019.

Saxton, W. A., & Schmitt, H. J. (1963) Transients in a large wave guide. *Proceedings of the Institute of Electrical and Electronics Engineers*, 51(2), 405-406.

Seybold, J. S. (2005). Introduction to RF propagation published by John Wiley & Sons, Inc., Hoboken, New Jersey.

Smith, E. K., & Weintraub D. S. (1953). The constants in the equation for atmospheric refractive index at radio frequencies. *Proceedings of the Institute of Radio Engineers*, 41(8), 1035-1037.

Troposphere https://en.m.wikipedia.org/wiki/troposphere retrieved on 15th September, 2020.

Wave propagation. Propagation of a radio wave https://www.tutorialspoint.com/what-are-the-methods-of-propagation-of-a-radio-wave retrieved on 22nd January 2019.

Willoughby, A. A., Aro, T. O., Owolabi, I. E. (2002). Seasonal variations of radio refractivity gradients in Nigeria. *Journal of Atmospheric Solar–Terrestrial Physics*, 64(4), 417-425.

Wyer, S. S. (1906). A treatise on producer-gas and gas-producer. Engineering and Mining Company., New York, USA.

Yola https://en.wikipedia.org/wiki/Yola,_Nigeria retrieved on 19th May, 2020.

APPENDIX A

Table 4.1: Hourly radio refractivity for typical dry season months in Bauchi (2012-2016)

LT (hr)	JANUARY	DECEMBER
12:00 AM	269	275
1:00 AM	270	276
2:00 AM	270	276
3:00 AM	271	276
4:00 AM	272	277
5:00 AM	274	278
6:00 AM	264	279
7:00 AM	275	279
8:00 AM	272	274
9:00 AM	266	269
10:00 AM	264	267
11:00 AM	262	265
12:00 PM	261	263
1:00 PM	260	263
2:00 PM	259	262
3:00 PM	258	262
4:00 PM	258	262
5:00 PM	258	263
6:00 PM	260	266
7:00 PM	264	270
8:00 PM	266	272
9:00 PM	268	273
10:00 PM	269	274
11:00 PM	269	274

Table 4.2: Hourly radio refractivity for typical wet season months in Bauchi (2012-2016)

MONTHS	JULY	AUGUST
12:00 AM	330	339
1:00 AM	331	338
2:00 AM	332	338
3:00 AM	331	339
4:00 AM	332	339
5:00 AM	333	338
6:00 AM	334	338
7:00 AM	334	338
8:00 AM	330	337
9:00 AM	327	335
10:00 AM	322	333
11:00 AM	318	331
12:00 PM	313	330
1:00 PM	309	328
2:00 PM	306	327
3:00 PM	303	326
4:00 PM	303	325
5:00 PM	305	328
6:00 PM	310	331
7:00 PM	316	336
8:00 PM	320	338
9:00 PM	325	339
10:00 PM	328	339
11:00 PM	330	339

Table 4.3: Hourly radio refractivity for typical dry season months in Yola (2012-2016)

LT (hr)	JANUARY	DECEMBER
12:00 AM	281	285
1:00 AM	282	284
2:00 AM	282	285
3:00 AM	283	285
4:00 AM	284	285
5:00 AM	285	285
6:00 AM	286	288
7:00 AM	284	288
8:00 AM	281	287
9:00 AM	279	284
10:00 AM	279	281
11:00 AM	276	279
12:00 PM	272	275
1:00 PM	271	274
2:00 PM	270	273
3:00 PM	270	272
4:00 PM	271	273
5:00 PM	276	275
6:00 PM	279	281
7:00 PM	280	284
8:00 PM	281	287
9:00 PM	282	287
10:00 PM	281	287
11:00 PM	281	286

Table 4.4: Hourly radio refractivity for typical wet season months in Yola (2012-2016)

LT (hr)	JULY	AUGUST
12:00AM	345	355
1:00 AM	344	355
2:00 AM	347	354
3:00 AM	348	354
4:00 AM	350	355
5:00 AM	350	356
6:00 AM	352	355
7:00 AM	351	354
8:00 AM	350	353
9:00 AM	349	351
10:00AM	347	350
11:00AM	342	349
12:00PM	338	345
1:00 PM	335	342
2:00 PM	321	340
3:00 PM	328	339
4:00 PM	328	327
5:00 PM	330	339
6:00 PM	333	342
7:00 PM	336	347
8:00 PM	339	349
9:00 PM	331	352
10:00PM	343	353
11:00PM	345	353

Table 4.5: Mean hourly radio refractivity for dry and wet season months in Bauchi (2012-2016)

LT (hr)	WET SEASON	DRY SEASON
12:00 AM	334	272
1:00 AM	334	273
2:00 AM	335	273
3:00 AM	335	274
4:00 AM	335	274
5:00 AM	335	276
6:00 AM	336	272
7:00 AM	336	272
8:00 AM	334	273
9:00 AM	331	268
10:00 AM	327	266
11:00 AM	324	264
12:00 PM	320	262
1:00 PM	318	261
2:00 PM	317	260
3:00 PM	314	260
4:00 PM	314	260
5:00 PM	317	261
6:00 PM	320	263
7:00 PM	324	267
8:00 PM	329	269
9:00 PM	332	270
10:00 PM	333	271
11:00 PM	335	272

Table 4.6: Mean hourly radio refractivity for dry and wet season months in Yola (2012-2016)

LT (hr)	WET SEASON	DRY SEASON
12:00 AM	350	283
1:00 AM	350	283
2:00 AM	351	284
3:00 AM	351	284
4:00 AM	352	284
5:00 AM	353	285
6:00 AM	354	287
7:00 AM	352	286
8:00 AM	352	284
9:00 AM	350	282
10:00 AM	348	280
11:00 AM	345	278
12:00 PM	342	274
1:00 PM	338	272
2:00 PM	331	272
3:00 PM	334	271
4:00 PM	328	272
5:00 PM	334	276
6:00 PM	337	280
7:00 PM	341	282
8:00 PM	344	284
9:00 PM	341	285
10:00 PM	348	284
11:00 PM	349	283

Table 4.7: Monthly variation of radio refractivity in Bauchi (2012-2016)

MONTHS	2012	2013	2014	2015	2016
JAN	258	266	266	272	276
FEB	269	263	261	256	252
MAR	253	274	268	281	288
APR	249	301	263	285	292
MAY	320	322	304	300	292
JUN	327	327	329	329	329
JUL	334	334	334	334	334
AUG	338	337	339	339	340
SEP	336	334	337	336	337
OCT	316	318	328	333	339
NOV	277	282	280	282	283
DEC	274	271	270	267	265

Table 4.8: Monthly variation of radio refractivity in Yola (2012-2016)

MONTHS	2012	2013	2014	2015	2016
JAN	279	279	279	279	49
FEB	279	290	284	284	53
MAR	283	278	270	277	120
APR	309	302	324	309	137
MAY	346	342	343	319	155
JUN	343	349	351	356	160
JUL	353	353	356	354	163
AUG	356	358	357	357	165
SEP	353	351	358	355	163
OCT	351	339	354	326	115
NOV	321	282	320	308	70
DEC	282	281	288	284	72

Table 4.9: Monthly variation of radio refractivity in Kano (2012-2016)

MONTHS	1.5 km	3 km	6 km	8 km
JAN	239	196	148	118
FEB	237	200	147	119
MAR	245	200	148	120
APR	250	204	147	120
MAY	261	211	149	120
JUN	270	216	153	121
JUL	276	222	154	121
AUG	283	226	155	122
SEP	277	220	152	122
OCT	260	212	148	121
NOV	247	205	148	120
DEC	238	201	147	121

Table 4.10: Mean monthly radio refractivity in Yola, Bauchi and Kano (2012-2016)

MONTHS	YOLA	KANO	BAUCHI
JAN	233	196	268
FEB	238	200	260
MAR	246	200	273
APR	276	204	278
MAY	301	211	308
JUN	312	216	328
JUL	316	222	334
AUG	319	226	339
SEP	316	220	336
OCT	299	212	327
NOV	260	205	281
DEC	290	201	269

APPENDIX B

Table 4.11: Mean seasonal variation of modified radio refractivity in Bauchi (2012-2016)

MONTHS	2012	2013	2014	2015	2016
JAN	355	363	363	369	373
FEB	365	360	358	353	349
MAR	350	371	365	377	385
APR	346	398	360	382	389
MAY	417	419	401	397	389
JUN	424	424	425	426	426
JUL	431	431	431	431	431
AUG	435	434	436	436	437
SEP	433	431	433	433	434
OCT	413	415	425	430	435
NOV	374	379	376	379	380
DEC	371	367	367	364	362

Table 4.12: Mean seasonal variation of modified radio refractivity in Yola (2012-2016)

MONTHS	2012	2013	2014	2015	2016
JAN	373	373	373	373	143
FEB	373	384	378	378	147
MAR	377	372	364	371	214
APR	403	396	418	403	231
MAY	440	436	437	413	249
JUN	437	443	445	450	254
JUL	447	447	450	448	257
AUG	450	452	451	451	259
SEP	447	445	452	449	257
OCT	452	433	451	420	209

NOV	415	376	414	402	164
DEC	376	375	382	378	166

Table 4.13: Mean seasonal variation of modified radio refractivity in Kano (2012-2016)

MONTHS	1.5 km	3 km	6 km	8 km
JAN	315	271	223	193
FEB	313	275	223	194
MAR	321	276	223	195
APR	326	279	222	195
MAY	337	286	224	196
JUN	345	291	228	196
JUL	351	297	230	196
AUG	358	301	231	197
SEP	352	295	228	197
OCT	336	287	224	196
NOV	322	281	223	196
DEC	313	277	222	196

APPENDIX C

Table 4.14: Mean monthly variation of radio refractivity gradient in Bauchi (2012-2016)

MONTHS	2012	2013	2014	2015	2016
JAN	-87	-89	-89	-89	-88
FEB	-85	-88	-87	-88	-89
MAR	-86	-86	-89	-91	-92
APR	-86	-97	-88	-92	-93
MAY	-107	-106	-101	-100	-97
JUN	-109	-109	-110	-110	-110
JUL	-94	-96	-111	-118	-127
AUG	-112	-112	-113	-113	-114
SEP	-94	-111	-112	-124	-133
OCT	-107	-111	-109	-111	-112
NOV	-92	-94	-93	-94	-95
DEC	-92	-91	-90	-89	-88

Table 4.15: Mean monthly variation of radio refractivity gradient over Yola (2012-2016)

MONTHS	2012	2013	2014	2015	2016
JAN	-93	-93	-93	-93	-16
FEB	-93	-97	-95	-97	-18
MAR	-94	-93	-90	-88	-40
APR	-103	-101	-108	-109	-46
MAY	-115	-114	-114	-106	-52
JUN	-116	-116	-117	-118	-53
JUL	-116	-118	-119	-120	-54
AUG	-117	-118	-119	-121	-55
SEP	-116	-116	-119	-117	-54
OCT	-111	-103	-119	-82	-38

NOV	-107	-94	-107	-26	-23
DEC	-94	-94	-96	-18	-24

Table 4.16: Mean monthly variations of radio refractivity gradient over Kano (2012-2016)

MONTHS	3 km	6 km	8 km
JAN	-29	-14	-8
FEB	-25	-14	-8
MAR	-30	-14	-7
APR	-31	-15	-7
MAY	-34	-16	-8
JUN	-36	-17	-9
JUL	-36	-17	-9
AUG	-38	-18	-9
SEP	-38	-18	-9
OCT	-33	-16	-8
NOV	-27	-15	-7
DEC	-24	-14	-7

APPENDIX D

Table 4.17: Variation of mean monthly radio refractivity and k-factor over Bauchi for 2012-2016

MONTHS	K-FACTOR	RADIO REFRACTIVITY
JAN	1.56	268
FEB	1.56	260
MAR	1.57	273
APR	1.58	278
MAY	1.65	308
JUN	1.70	328
JUL	1.70	334
AUG	1.72	339
SEP	1.73	336
OCT	1.70	327
NOV	1.60	281
DEC	1.57	269

Table 4.18: Variation of mean monthly radio refractivity and k-factor over Yola for 2012-2016

MONTHS	K-FACTOR	RADIO REFRACTIVITY
JAN	1.49	233
FEB	1.51	238
MAR	1.52	246
APR	1.59	276
MAY	1.64	301
JUN	1.66	312

JUL	1.67	316
AUG	1.68	319
SEP	1.67	316
OCT	1.58	299
NOV	1.45	260
DEC	1.42	290

Table 4.19: Variation of mean monthly radio refractivity and k-factor over Kano for 2012-2016

MONTHS	K-FACTOR	RADIO REFRACTIVITY
JAN	1.24	196
FEB	1.19	200
MAR	1.24	200
APR	1.25	204
MAY	1.27	211
JUN	1.30	216
JUL	1.30	222
AUG	1.32	226
SEP	1.32	220
OCT	1.26	212
NOV	1.21	205
DEC	1.18	201

Table 4.20: Mean monthly k-factor variations in Bauchi, Kano and Yola (2012-2016)

MONTHS	KANO	BAUCHI	YOLA
JAN	1.24	1.56	1.49
FEB	1.19	1.56	1.51
MAR	1.24	1.57	1.52

APR	1.25	1.58	1.59
MAY	1.27	1.65	1.64
JUN	1.30	1.70	1.66
JUL	1.30	1.70	1.67
AUG	1.32	1.72	1.68
SEP	1.32	1.73	1.67
OCT	1.26	1.70	1.58
NOV	1.21	1.60	1.45
DEC	1.18	1.57	1.42

APPENDIX E

Table 4.21: Mean monthly field strength variability over Bauchi (2012-2016)

MONTHS	FSV
JAN	8
FEB	12
MAR	12
APR	17
MAY	14
JUN	12
JUL	11
AUG	8
SEP	11
OCT	13
NOV	16
DEC	7

Table 4.22: Mean monthly field strength variability over Yola (2012-2016)

MONTHS	FSV
JAN	13
FEB	18
MAR	21
APR	22
MAY	17
JUN	13
JUL	13
AUG	10

SEP	13
OCT	15
NOV	17
DEC	12

Table 4.23: Mean monthly field strength variability over Kano (2012-2016)

MONTHS	FSV
JAN	3
FEB	3
MAR	4
APR	4
MAY	3
JUN	3
JUL	3
AUG	3
SEP	2
OCT	2
NOV	3
DEC	3